Decouple and Control Strategy for Variable Speed Variable Pitch Wind Energy Conversion System

A THESIS
SUBMITTED TO THE FACULTY OF THE GRADUATE SCHOOL
OF THE UNIVERSITY OF MINNESOTA
BY

Shanmukha Reddy Modugula

IN PARTIAL FULFILLMENT OF THE REQUIREMENTS
FOR THE DEGREE OF
MASTER OF SCIENCE

Prof Dr. Desineni Subbaram Naidu

March 2018

Acknowledgements

This document is the result of two and a half years of research, training and guidance of **Prof. Dr.Subbaram Naidu** my adviser whom I am really grateful for providing me with very much needed motivation and support by helping me understand some advanced concepts for fulfilling this research and also helping by introducing me to some great minds like **Dr.Hoa Minh Nguyen,Tsungai Chibanga and Neng Wan** when I needed help for understanding difficult parts of my research. I am very thankful for all these great people who have helped me solve some difficult difficult problems with my research work.

As an international student I really had a great time at **University of Minnesota Duluth** which has provided me with great opportunities all along and the inclusiveness of people with other fields of study has helped me academically and personally to take a step towards research work. And also the faculty of my department (Department of Electrical Engineering) were helpful in deciding my field of interest and encouraging me for this research study all along. And I would like to say a special thanks to **Shey Peterson** Administrative Secretary of Electrical Engineering Department was helping me with all the formalities and was very kind to me when I first came to UMD. It is difficult to mention all the people who have been a great help during the great journey at university that I am thankful to but I will alwyas be thankful to those.

Abstract

With the rapid growth of wind energy usage, the complexity of control systems used in the wind energy conversion systems (WECS) is also growing. As the nature of the wind is indeterminate, control systems must be able to deal with the stochastic nature of the wind and must be able to give the desired results. Thus, consideration of different types of advanced controllers for the WECS becomes important. One of the promising divide (decouple) and conquer (control) strategy using singular perturbations and time scales (SPaTS) for WECS has been used earlier for variable speed and constant pitch (VS-CP) wind model and using the linearization of the nonlinear model.

In this project, the model of the variable speed and variable pitch (VS-VP) turbine wind energy system is considered for study. The designing and integrating the model of the VS-VP system is a bit more complicated and challenging than that of the VS-CP model. Further, the VS-VP system contains both mechanical and electrical components giving rise to the slow and fast dynamics, respectively and hence exhibiting the time scales. Briefly, the SPaTS technique helps in expressing the system with low-order, outer (slow) dynamics and inner (fast) dynamics. The inner dynamics is also called boundary layer correction. In this project we consider VS-VP WECS model for the decoupling process to obtain low-order slow and fast subsystems. Next, using the advanced optimal control methods, two low-order, closed-loop, optimal, slow and fast sub-controllers are obtained. A composite optimal controller is constructed using the two slow and fast sub-controllers and applied to the original nonlinear wind energy system. Comparisons are made between the results of the system using the full-order, optimal controller and the low-order, optimal sub-controllers to validate the SPaTS strategy.Finally, some conclusions and future work are included.

Contents

Contents iii

List of Tables vi

List of Figures vii

1 Introduction 1

1.1 Wind Energy 1

1.1.1 Wind Behavior 2

1.1.2 Advantages and Disadvantages of Wind Energy 5

1.1.3 Wind Energy Developments 7

1.2 Wind Energy Conversion Systems 9

1.2.1 Composition of Different Parts of WECS 10

1.2.2 Different Subsystems of WECS 11

1.2.3 Different Types of WECS 13

1.3 Literature Survey 17

1.3.1 Hard Control 18

1.4 Problem Statement 25

1.5 Research Objectives 26

1.6 Overview 28

2 Dynamic modeling of Wind Energy Conversion System **29**

2.1 Introduction 29

2.2 Aerodynamic Subsystem Modelling 30

2.3 Drive Train Subsystem Modelling 32

2.3.1 Drive Train Dynamics 33

2.4 Generator Modelling 35

2.5 Pitch Subsystem Modelling 37

2.6 Non-linear Model of the Entire WECS 38

2.7 Linearized Model 39

2.8 Chapter Summary 41

3 Singular Perturbation and Time Scales Analysis and Synthesis **42**

3.1 Introduction 42

3.2 Time Scales Derivation 43

3.2.1 Block Diagonalization Technique 43

3.2.2 Recursive Algorithms 48

3.3 Time Scale Analysis of a Grid-Connected PMSG Based WECS 50

3.4 Decoupling Results 56

3.5 Chapter Summary 57

4 Analysis and Design of VS-VP System **59**

4.1 Introduction 59

4.2 Optimal Linear Quadratic Regulator (LQR) Control 59

4.2.1 Optimal LQR Filter Design for the Original System 59

4.2.2 Optimal LQR Filter Design for the Slow Subsystem 61

4.2.3 Optimal LQR Filter Design for the Fast Subsystem 62

4.3 Optimal Linear Quadratic Guassian (LQG) Control 64

4.3.1 Decoupling Kalman Filter Design 65
4.3.2 Optimal LQG Control Design 70
4.4 Summary 73

5 Results **74**
5.1 Introduction 74
5.2 Optimal LQR Control Simulation Results 74
5.2.1 Optimal LQR Control and Simulation Results for Original System 75
5.2.2 Optimal LQR Control and Simulation Results for Slow and Fast Subsystems 76
5.2.3 Comparision of Responses of Each State 78
5.3 Optimal LQG Control Simulation Results 79
5.3.1 Optimal LQG Control Simulation Results 80

6 Conclusions and Future Works **99**
6.1 Conclusion 99
6.2 Future Works 100

References **102**

List of Tables

3.1 Grid-connected PMSG based WECS 51

3.2 Eigen value comparision of Original system and Decomposed subsystems 57

List of Figures

1.1 Wind Spectrum [12] 2
1.2 Weibull Probability Distribution of Wind Speed [14] 4
1.3 Power Density vs average Wind Speed [14] 4
1.4 Global Annual Installed Wind Capacity 2000-2015 [8] 8
1.5 Global Cumulative Installed Wind Capacity 2000-2015 [8] 8
1.6 Cumulative capacity by Country 2015 [8] 9
1.7 Different Parts of a Wind Turbine [11] 11
1.8 HAWT and VAWT [11] 14

2.1 WECS Subsystems Modelling and Classification 29
2.2 Aerodynamic Subsystem 30
2.3 Drive Train Subsystem 33
2.4 Drive Train Diagram 34
2.5 PMSG equivalent circuit diagram. (a) d-axis equivalent (b) q-axis equivalent 35
2.6 Pitch System 37

3.1 Time Scale LQR control diagram 47
3.2 Eigen Values Plot 54

4.1 Time Scale LQR control diagram 64
4.2 LQG Control Diagram 73

5.1 LQR Original System Results 76
5.2 LQR Decoupled System Results 78
5.3 Comparision of Angular Velocity of Rotor (ω_r) 79
5.4 Comparision of Angular Velocity of Generator (ω_g) 79
5.5 Comparision of Internal Torque (T_H) 80
5.6 Comparision of Pitch Angle (β) 80
5.7 Comparision of d-component of stator current in PMSG (i_d) 81
5.8 Comparision of q-component of stator current in PMSG (i_q) 81
5.9 State Estimates for LQG Original System (i_q) 85
5.10 Response for (ω_r) original system 86
5.11 Response for (ω_r) decomposed system 86
5.12 Difference between the Responses for (ω_r) 87
5.13 Difference between the Control signals for ω_r 87
5.14 Response for (ω_g) original system 88
5.15 Response for (ω_g) decomposed system 89
5.16 Difference between the Responses for (ω_g) 89
5.17 Difference between the Control signals for ω_g 90
5.18 Response for (T_H) original system 90
5.19 Response for (T_H) decomposed system 91
5.20 Difference between the Responses for (T_H) 91
5.21 Difference between the Control signals for (T_H) 92
5.22 Response for (β) original system 92
5.23 Response for (β) decomposed system 93

5.24 Difference between the Responses for (β) 93
5.25 Difference between the Control signals for (β) 94
5.26 Response for (i_d) original system 94
5.27 Response for (i_d) decomposed system 95
5.28 Difference between the Responses for (i_d)) 95
5.29 Difference between the Control signals for (i_d) 96
5.30 Response for (i_q) original system 96
5.31 Response for (i_q) decomposed system 97
5.32 Difference between the Responses for (i_q)) 97
5.33 Difference between the Control signals for (i_q) 98

1 Introduction

This chapter discusses and gives an outline about the importance about wind energy and a general overview of the WECS. It explains about different types of WECS, the issues with WECS and the recent developments related to the WECS, followed by the literature survey of advanced control strategies for the WECS. Towards the end of chapter, a control problem for VSVP WECS are addressed and the objectives of this research project are sorted out.

1.1 Wind Energy

The wind energy is one of the sustainable sources of energy and is considered clean as there is no air, water or land pollution that is created to produce wind energy. Humans have been using the wind energy from a very long time, ancient mariners used sails to capture the wind and explore the world. Farmers once used windmills to grind their grains and pump water. Today, more and more people are using wind turbines to wring electricity from the breeze. Over the past decade, wind turbine use has increased at more than 25 percent a year [8]. Still, it only provides a small fraction of the world's energy. With the rising issue of climate change which is a global problem, the need to change the energy sources from Conventional energy sources (Coal, Natural gas etc.) to Sustainable energy sources is more imminent. Though there are many Sustainable energy sources like Solar, Hydro-Electric, Geothermal, Bio-fuel etc. solar and wind energy is more preferred over other options because these

are more affordable than others and can be scaled up as needed very easily. Wind energy is the fastest growing energy resource in the world. This research focuses on wind energy, so we will see more in depth study about wind energy.

1.1.1 Wind Behavior

We need to know how the wind varies at a site before installing a wind turbine which helps in estimating the power generated at that site also, turbine designers need the information to optimize the design of their turbines, so as to minimize generating costs. Turbine investors need the information to estimate their income from electricity generation. The wind velocity variations can be studied using three different time scales: large time scale, mean time scale and short time scale [5]. The large time scale wind study explains the wind variations from year to year, even decades. The mean time scale winds studies show the variations that occur seasonally so, it can be predicted accurately by using statistical data based on long observations of wind speed data at the required sites. Short time scale wind is called turbulence it represents the variations of wind from minutes to seconds.

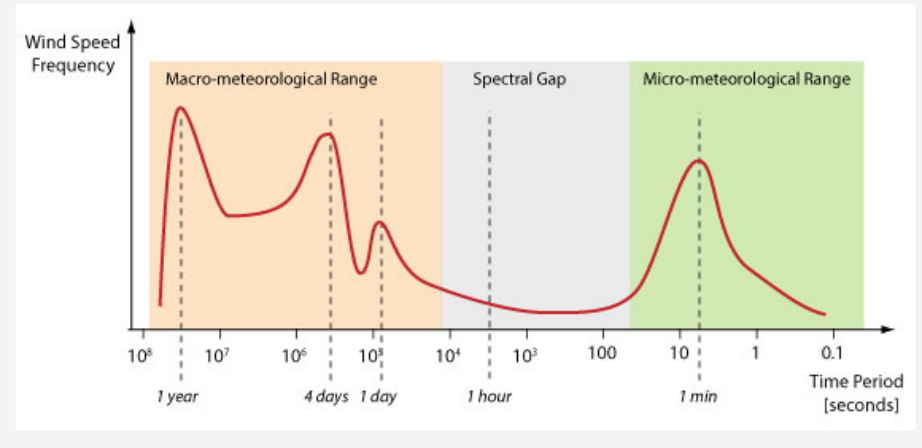

Figure 1.1: Wind Spectrum [12]

Above graph shows the wind spectrum, high value in the graph indicates high variations in the wind velocity corresponding to that time period. Though this graph is site specific it resembles few similarities. The different peaks in the above graph represent the annual, seasonal and daily turbulence in the wind. The 3 peaks in the macro meteorological range indicate the turbulence in Large time scale the main reason for these peaks are:

- Annual pattern: Which is due to the varying radiations of the sun due to revolution of earth around the sun. These patterns change with degrees of latitude and vanishes in close proximity of the earth.
- Depressions and Anti-Cyclones: This is due to changes in the pressures in atmosphere and it is more distinctive in Oceania than the continental regions. It usually occurs with a period of about 4 days.
- Diurnal Pattern: It is caused by variation in the temperatures at day and night. This effect is more distinct at the coastal region than the off-shores.

The peaks in the Micro meteorological range are due to the short time-scale, sometimes the wind velocity might double or triple in seconds, which in turn makes the power generated by wind turbine 8 times or 27 times (Power is proportional to cube of wind velocity) in matter of seconds. The turbulence scales up with the presence of obstacles like buildings, trees etc.

The spectral gap can be seen between 2 hours to 10 minutes region because there is not much turbulence in wind happening for every 2 hours or 1 hour periodically. The distribution of hourly average wind speeds can be represented by a Weibull distribution which is considered as mean time scale wind distribution. This distribution

is given by:

$$p(V_m) = \frac{k}{c}(\frac{V_m}{c})^{k-1}e^{(\frac{-V_m}{C})^k} \tag{1.1.1}$$

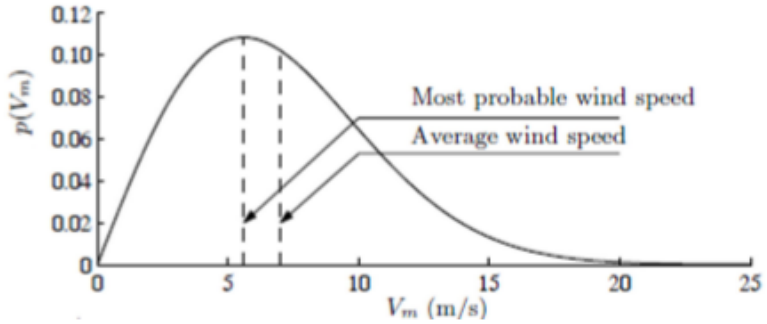

Figure 1.2: Weibull Probability Distribution of Wind Speed [14]

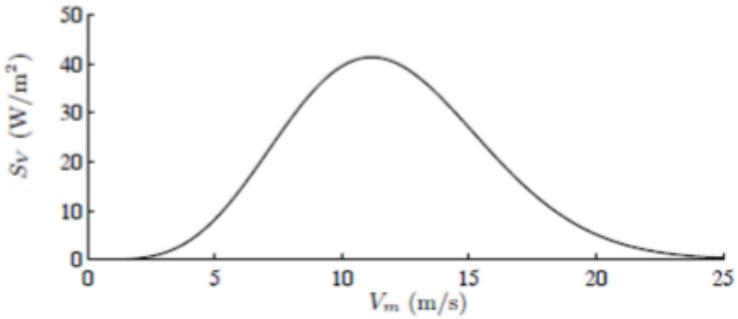

Figure 1.3: Power Density vs average Wind Speed [14]

V_m in the equation is mean wind speed and $p(V_m)$ is the probability distribution. k and c are the shape and scaling coefficients of the curve respectively, and these coefficients are adjusted to represent the wind data of that specific site. The graph from Fig 1.2 explains that the probability of high wind velocity and very low wind velocity is low as that occurs very rarely most probable wind speed is 5.5 m/sec which has occurred most frequently based on the statistical data and has the highest

probability to occur again at the site which the graph corresponds to. More important conclusion can be drawn from second graph in Fig 1.3 demonstrating power density versus speed, that there is higher power density at the wind velocities between 10 m/sec to 13 m/sec this is a very important fact to be noted which might help in deciding the placement of the WECS.

1.1.2 Advantages and Disadvantages of Wind Energy

Wind energy has many advantages to offer which explains why wind energy has the fastest growth of all the energy sources. Though there are many advantages there are also lot of challenges that it has to overcome. The advantages of wind energy are as follows [10, 48]:

- Renewable and sustainable: The wind itself is renewable and we never run out of wind unlike fossil fuel so the price of wind energy does not fluctuate as much as the fossil fuels making it an ideal sustainable power source.

- Eco-friendly: Wind energy is considered one of the most environmental friendly energy source. There is very little to no emission of harmful substances or greenhouse gases into atmosphere or the surrounding environment after the manufacturing and installation of the wind turbines. Though, there is noise pollution but it considered as environmental effect but there is no negative effect to earth, water or the air we breathe.

- Wind Energy is cheap: We can never run out of wind so there is an uninterrupted supply of wind of wind and it only costs us for the wind turbine, the site for the turbine and maintenance which is very less compared to the uninterrupted supply of the power we can tap from the wind energy. At times Wind energy was sold at price as low as 2.5 cents/KWh.

- Reduces Fossil fuel Consumption: Generating electricity from wind energy reduces the usage of fossils. This can help to conserve dwindling supplies of the earths natural resources, allowing them to last longer and help to support future generations.

- Remote power Solution: For the remote areas we do not need to generate energy elsewhere and transmit energy to remote areas from there through the lines.

- Increases energy security: By using wind energy we are reducing the dependency of power generation from the fossil fuels which are often sourced from other countries, due to which there are fluctuations of pricing in power generation. War, politics and overall demand often dictate the price for natural resources, which can fluctuate and cause serious economic problems or supply shortages for some countries. By using renewable energy sources a country can help to reduce its dependency on global markets and thus increase its energy security.

- Job creation: Wind energy industry has boomed ever since the wind turbines are available on the market. This has helped create jobs all over the world. There are many job created for manufacturing, maintain and installing the wind turbines and also in wind energy consulting, where specialist consultant will help in determining a wind turbine installment will generate a return on investment.

The challenges that the wind energy is facing are clearly outweighed by the advantages but lets just have a look at the challenges:

- Wind is intermittent: The wind does not always blow in the same way at any location. This is a serious problem for wind turbine developers who often invest a lot of time and money investigating whether a site is suitable for wind

generation. Thats is why we often see wind turbines built on top of hills or at the sea where there is no obstruction by land masses.

- Manufacturing and Installation is very expensive: Although costs are reducing, designing and installation of a turbine is costing a lot, site survey needs to be conducted at multiple locations for a significant amount of time and if deemed adequate the cost of laying foundation, transporting a huge turbine and erecting it at the site the overall cost is huge. If it is an off-shore wind turbine the cost for installing it is even higher.

- Threat to Wild Life: There have been many cases in Europe where a lot of birds and bats die. However, the threat due to the wind turbines is much less compared to the cell towers and radio towers. Nevertheless, wind turbines are contributing to the mortality rate of birds and bats population.

- Noise and Visual Pollution: There is a loud noise when the wind turbine is operating which is around 45 dB if the turbine is a mile away then the noise effect is negligible. Also the wind turbines when erected upon a hill the scenery might not always look nice.

- Radar Noise: When the wind turbine is installed near an air force or military base, the noise due to the turbine creates an interference due to which radar tracking becomes less efficient.

1.1.3 Wind Energy Developments

The wind energy is fastest growing in the energy sources because a lot of nations are their governments are investing in the wind energy a lot each and every year. It is understandable why wind energy is growing at an enormous rate looking at the

advantages stated earlier in this chapter. The recent statistics of new installations and the cumulative wind energy after Dec 2015 installed across the world can be seen in the graphs and charts [8] below:

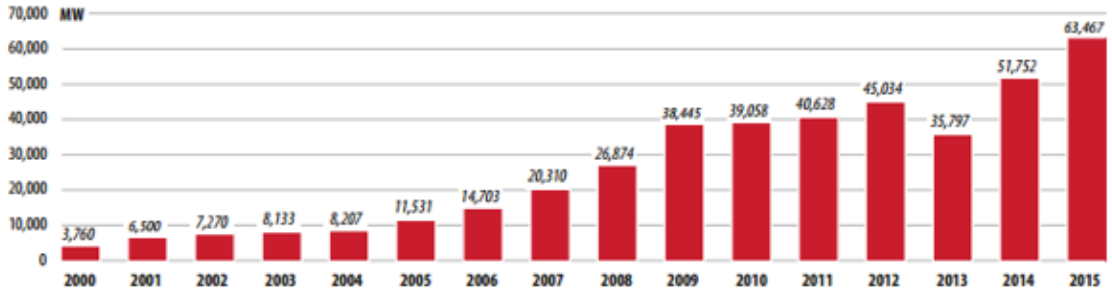

Figure 1.4: Global Annual Installed Wind Capacity 2000-2015 [8]

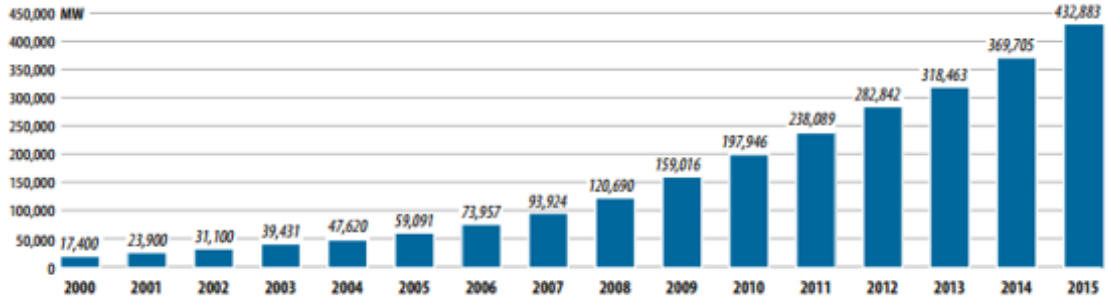

Figure 1.5: Global Cumulative Installed Wind Capacity 2000-2015 [8]

The above graph only shows the cumulative wind energy generated across the world and the country wise share of the wind energy production can be seen in the pie chart below by the end of the year 2015.

In the pie chart below, from the overall wind energy of 432,883 MW each country share is as follows: PR China with 33.6%, USA 17.2%, Germany 10.4%, India 5.8%, Spain 5.3%, United Kingdom 3.1%, Canada 2.6%, France 2.4%, Italy 2.1%, Brazil 2%, and the Rest of the World with 15.5%. In the recent years since 2010 a lot of money has been invested in wind by China where the wind energy is booming.

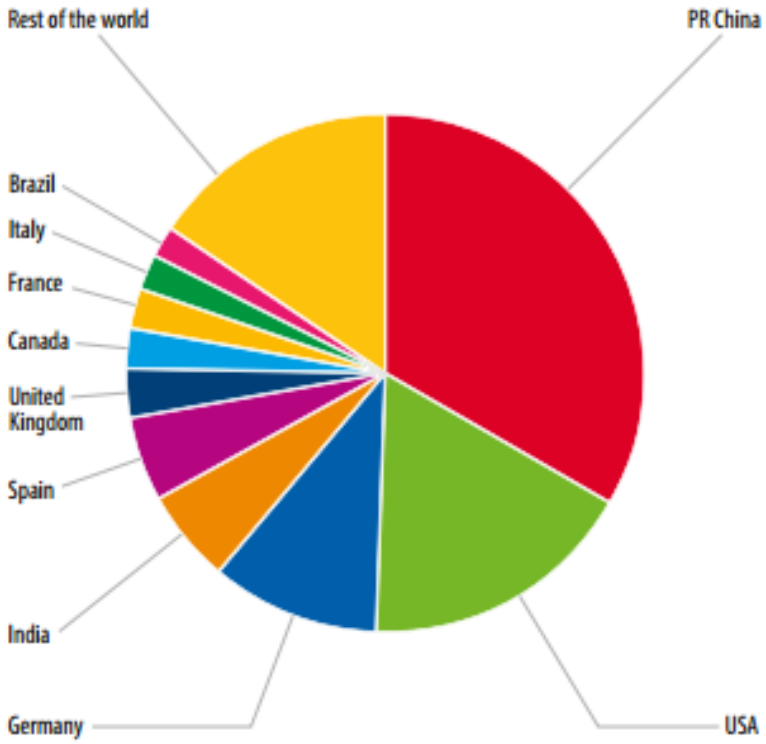

Figure 1.6: Cumulative capacity by Country 2015 [8]

The growth in United States has been steady and USA aims at reaching a target of 20% wind energy of total power needs by the end of 2025 which is currently 3.6% of the total power requirements. There has also been a lot of developments in the design of Wind Turbine, there are so many new models of wind turbines that have been invented to improve the efficiency of the wind turbines and there is still a lot of research still going on.

1.2 Wind Energy Conversion Systems

A Wind Energy Conversion System converts wind energy into electrical energy, to do that a wind turbine is used and there are many different devices used in the wind

turbine which are generally sub-divided into subsystems. To improve the efficiency of the WECS the design of each and every subsystem can be improved. There have been a lot of improvements in many subsystems due to the research being done on WECS from a very long time. In this section, we will discuss in brief about the different subsystems of WECS, different types of WECS and the most remarkable improvements in the WECS.

1.2.1 Composition of Different Parts of WECS

The basic parts of the wind turbine are the tower, blades, rotor shaft, gear-box, generator and regulator, additional parts can be added to improve the efficiency of the wind-turbines. The fundamental parts of a wind-turbine can be seen in the image Fig1.7 below. Generally, the dimensions of a wind-turbine vary with the purpose for which they have been installed [47]. Industrial wind turbines are lot bigger than the ones that you might find in the school back yard or behind someones house. Widely used GE 1.5MW model Wind Turbine consists of 116-ft blade atop a 212-ft tower for a total height of 328 feet. The blades sweep a vertical airspace of just under an acre. Whereas, the 1.8-megawatt Vestas V90 from Denmark has 148-ft blades (sweeping more than 1.5 acres) on a 262-ft tower, totaling 410 feet. Another model being seen more in the U.S. is the 2-megawatt Gamesa G87 from Spain, with 143-ft blades (just under 1.5 acres) on a 256-ft tower, totaling 399 feet. The huge turbines require a correspondingly large area around them clear of trees and other turbines to maximize the effect of the wind and avoid interference. They should have 10 rotor diameters of clearance in the direction of the wind and 3 rotor diameters in every other direction.

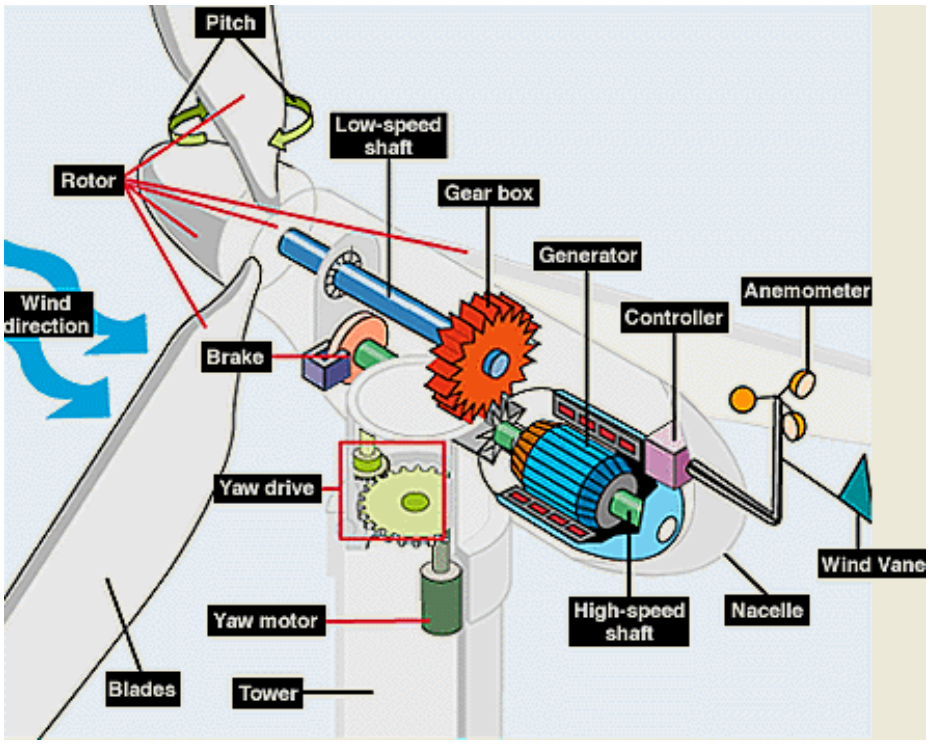

Figure 1.7: Different Parts of a Wind Turbine [11]

1.2.2 Different Subsystems of WECS

There are many different physical parts in the wind turbines, they are organized as different sub-systems which are inter-connected to each other to complete the WECS. They are divided into sub-systems with respect to energy conversion flow [11]. The different sub-systems in the WECS are as follows as shown in the fig 1.7:

1. Aerodynamic sub-system: It is used to convert the kinetic energy of the wind into Mechanical energy. This sub-system consists of Blades, Hub, and pitching devices used to change the alignment of the blades. When the wind cuts through the blades surface of the turbine it creates a lift force, due to which the blades connected to the hub start rotating the rotor in the hub. The pitching devices are used to adjust the amount of lift force that acts upon the blades, so that the speed of rotor can be varied, in this manner the rotor speed is controlled

through the pitching system. The rotor in the hub is connected to the drive train sub-system delivering the mechanical torque generated from the kinetic energy of the wind.

2. Drive-Train Sub-system: Drive-train sub-system is like a transmission system which takes the energy provided by the aerodynamic system and modifies it per the needs of the generator. The drive train sub-system has a gear mechanism which converts the high torque low speed provided by the aerodynamic sub-system into low torque high speed to the generator which is required by the generator.

3. Generator: Generator is an electro-mechanical transducer which converts the mechanical energy into electric energy. The power output from the wind-turbine mainly depends on the generator. So, Generator is one of the most important components of the wind turbine. There are many different types of Generators like Squirrel Cage Induction Generator (SCIG), Doubly Fed Induction Generator (DFIG), and Permanent Magnet Induction Generator(PMIG). Depending on the design the power generated by generators can be fed to the grid directly to the power-electronic convert which can control the power flow to the consumers directly.

4. Other subsystems: Other than the above mentioned three sub-systems there might be many other important sub-systems like the control-system block (which guide how to change the settings of the pitch system and direction of the facing of turbine etc.), yaw (used to change the direction of the rotor), brakes, wind vane (to know the direction of the wind), tower etc.

1.2.3 Different Types of WECS

WECS have been improved a lot from the past century and now there are many different types of WECS that exist today. A lot of advancements have been made in the design and performance of the WECS, starting from the small and simple to large and complex with respect to the size, efficiency, power generated and Control System. There are many different classifications of WECS [11] that exist today. The classifications can be made based on the wind rotor axis, based on the controls used on the turbine, based on the location of the turbine, based on the connectivity and many more types of classifications.

1. Depending on wind rotor axis [41] there are two different types of Wind Turbines as shown in Figure 1.8:

    - *Horizontal Axis Wind Turbines (HAWT):* The axis of rotation of the rotor is horizontal with respect to the ground and are the common style that most of us think of when we think of a wind turbine. Horizontal axis wind turbines have the main rotor shaft and electrical generator at the top of a tower, and they must be pointed into the wind. Small turbines are pointed by a simple wind vane placed square with the rotor (blades), while large turbines generally use a wind sensor coupled with a servo motor to turn the turbine into the wind. Since a tower produces turbulence behind it, the turbine is usually pointed upwind of the tower.
    - *Vertical Axis Wind Turbines (VAWT):* VAWTs, have the main rotor shaft arranged vertically. The main advantage of this arrangement is that the wind turbine does not need to be pointed into the wind. This is an advantage on sites where the wind direction is highly variable or has turbulent winds. With a vertical axis, the generator and other primary components

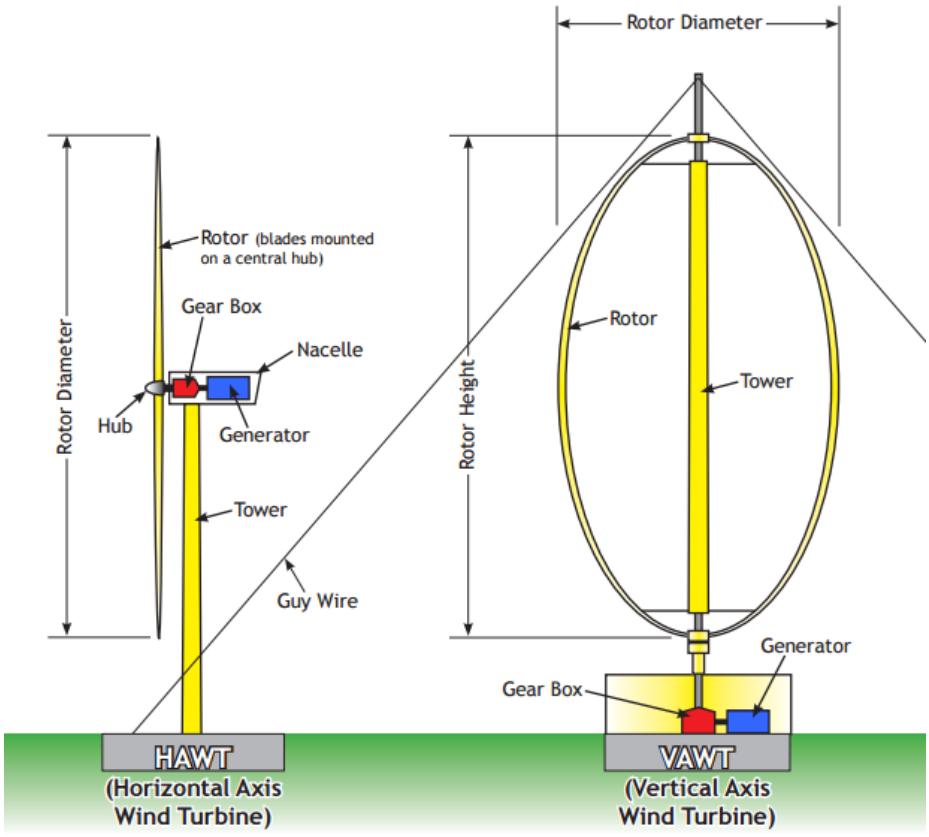

Figure 1.8: HAWT and VAWT [11]

can be placed near the ground, so the tower does not need to support it, also makes maintenance easier. It is difficult to mount vertical-axis turbines on towers, meaning they are often installed nearer to the base on which they rest, such as the ground or a building rooftop. The wind speed is slower at a lower altitude, so less wind energy is available for a given size turbine. Air flow near the ground and other objects can create turbulent flow, which can introduce issues of vibration, including noise and bearing wear which may increase the maintenance or shorten its service life. However, when a turbine is mounted on a rooftop, the building generally redirects wind over the roof and this can double the wind speed at the tur-

bine. If the height of the rooftop mounted turbine tower is approximately 50% of the building height, this is near the optimum for maximum wind energy and minimum wind turbulence.

2. Depending on the location there are two different types of the Wind Turbines.

   - *On-shore Wind Turbines:* On-shore Wind Turbines are land based wind turbines which are set up on land, which consume a huge land area and generate a lot of noise pollution, visual pollution and harm to birds [11]. However, there are also many cost benefits to onshore wind power that by extension impact the environment. Onshore wind often has the benefit of being close to existing electrical grids, reducing the environmental impacts associated with building new electrical grids.
   - *Off-shore wind turbines:* Off-shore wind turbines are installed right off the coasts or little further away from the coasts in sea. The advantages are huge as it does not require any land resources and there will be no noise pollution or environmental effect to the birds. Wind turbines are placed on concrete platforms that extend to the bottom of the sea, and further out in the sea using floating platforms, increasing costs through additional materials and for installing the dedicated power grid. One of the most important environmental aspects of wind power is the low pay-back time. For a 40.5m Wind Turbine, based on a 40% estimated efficiency, the payback time becomes 0.39 years, less than 2% of the 20-year life span of an offshore wind farm [11].

3. There are two types of wind farms with respect to their connectivity

   - *Stand Alone Wind farms:* Power through the power grid is not available in

some rural and isolated regions, in such cases the power to places like those are provided by Wind Turbines, farms or Hybrid System. Their power is only limited to the local grid.

- *Grid Connected Wind Farms:* To diversify the power sources and to get cheaper electric power Wind Farms are integrated to the existing power grids. This kind of installation is more dominant these days.

4. There are four different types of wind Turbines depending on the control point of View:

   Using the fundamental Control Techniques either the Speed can be controlled or the output power generated by the turbine can be controlled. Depending on the design of the generator and wind turbine the speed can either be controlled or nor controlled, resulting in two variations of speed control namely, Fixed-speed and Variable-speed, respectively. Speed Control can be used to maximize the power conversion as by controlling the speed of generator the turbine can be maintained at optimal conditions. Power control refers to how to control the aerodynamic efficiency to control the converted power when the wind speeds are large and above the rated capacity of the Wind Turbines. Controlling the aerodynamic efficiency can be achieved by controlling the orientation of the pitch angle of the blades of turbine so that the effect of the wind on the blades can vary, this type of control is called active power control or variable-pitch power control. There is also a simpler way called passive or fixed-pitch power control, which is implemented by special design of blades such that they can be stalled at high wind speeds to reduce the aerodynamic effect. However, the fixed-pitch technique has a drawback that it produces an immense stress on the wind turbine which might reduce the life time of a turbine and increasing the

maintenance costs of turbine. Now by combining both the control technologies together four different types of types of win turbines can be designed:

- Fixed-speed Fixed-pitch (FSFP) wind turbines.
- Fixed-speed Variable-pitch (FSVP) wind turbines.
- Variable-speed Fixed-pitch (VSFP) wind turbines.
- Variable-speed Variable-pitch (VSVP) wind turbines.

1.3 Literature Survey

It is important to get an overview of State-of-the-art study of WECS for this research project, as there have been many recent literature reviews concerning the topics related to this research project on many different aspects of the WECS. Like the publication [13] deals with the Low-voltage ride through problem which is one of the biggest challenges faced by massive deployment of wind farms especially when they are grid-connected, which are becoming more popular these days. The report in [39] gives a study to determine the placement of the off-shore wind turbines using a new search algorithm. In [7] authors review many recent advancements and existing concepts, state of the art and theories in the power-electronic systems related to the wind turbine. The study to monitor the condition and health of the WECS using the different sensors connected to the turbine is summarized in [20]. Optimal Voltage control of the instabilities in uncertain voltage output is presented in detail in [50]. An overview of WECS developments, technologies and power electronics research trends is demonstrated in [43]. In a study [4] different types of generators for WECS topology was reported. In [36] the author gives an overview and emphasizes on hard and soft computing techniques for control design purpose, as well as eects

of hybrid techniques. The details of the overview on different control techniques are presented in this section. The different types of control techniques and a brief insight about each type of control technique will be given in this section.

1.3.1 Hard Control

Hard control techniques use Hard computing, (i.e., conventional computing), which requires a precisely stated analytic model and often a lot of computation time. It cannot deal with imprecision and approximation. Most widely used Hard control techniques in control theory are PID control, Optimal Control, Adaptive Control, Sliding mode control and Predictive control.

PID Control:

The study of using PID control in WECS has been done by many people and is being done from a very long time. Either the pitch control or the Speed control of the WECS can be performed using the PID technique. Power control or Speed control of WECS using PID and using PID along with other control in hybrid controls techniques was proposed in [28], [15], [3] . In [3] an expert PID controller is designed for variable speed and variable pitch wind turbine, which is based on the tracking-differentiator. The tracking-differentiator is used to arrange transitions of the control variables, such as the rotor speed, and reasonably extract the one-order differential signal from the speed deviation. The inputs of the expert PID controller are the speed deviation and its one-order differential signal. The proposed method is compared with the conventional PI control strategy. It is shown that the performance of the expert PID controller is satisfactory and the proposed method is feasible also, it can cope with the nonlinear characteristics of wind turbines. In [28], an intelligent PID(iPID)

technique was used to improve the efficiency for tracking of the Maximum Power Point(MPP). The principle of iPID control strategy for power utilizes an observer to estimate disturbance including the internal and external factors online. The core issue of this method is to obtain disturbance effectively. However, the iPID technique cannot deal with the errors and disturbances very well, the approximated error is treated same as the last two sampling time error. When reference is a high-frequency signal, the equivalence relationship will be not satisfied. The noise of sensors also will increase the error and worsen the performance of the control technique. Considering the estimated error of disturbance, an additional sliding model controller is proposed. The extra controller compensates for estimated error. And according to Lyapunov stability theory, this sliding model controller ensures the closed-loop stability in wind turbine system. In depth study about iPID control is done in [15].

Optimal Control:

Optimal control is generally used for optimizing a cost function, Energy function or an efficiency function which is generally power (i.e.; energy function) in the case of WECS, as concerned to this research. In WECS optimal control is usually used for pitch control to improve the conversion efficiency of WECS, sometimes it is used in combination with other control techniques as per the requirements [9].

Optimal control techniques used in this dissertation are from [22] which are used for Linearizing a Non-linear WECS model and the MPPT technique. In [30], optimal control technique was applied on variable speed wind turbine under dynamic wind conditions to increase the energy efficiency. The results are verified both by simulation and laboratory experiments using a model turbine systems, and show that a 9 to 15% improvement in net energy extraction from the wind is achievable. Authors explains how a squirrel cage induction generator can be controlled using a PWM voltage source

inverter and a simple speed controller to maintain optimum power transfer conditions for the wind turbine in varying wind speed conditions. The main limit to the ability of the system to follow the changes in wind speed is the large rotor inertia preventing the rapid acceleration of the rotor. Much greater efficiency have also been shown to be obtainable by optimizing the generator excitation for operating conditions. [27], [45], [29] give an overview of the new developments in optimal control. [27] is a recent study of optimal control of variable speed wind turbine based on extreme learning machine and adaptive particle swarm optimization, where a machine learning algorithm is used to optimize the control algorithm according to the non-linearities. Main objectives of the study are to maximize the energy conversion and to maintain the safety of Wind Turbines by reducing the stress on drive train shafts. Extreme Learning Machine algorithm with high learning speed is used to approximate the error in case of unmodeled non-linear dynamics, while the Sliding Mode Control is used to compensate for the external disturbances and modelled errors. Adaptive Particle Swarm Optimization algorithm is introduced to adapt and optimize the gain of the Sliding Mode Control as per the information learned by the Extreme Learning Machine. The proposed method in the study is illustrated in simulations by comparing it with the traditional Sliding Mode Control. Optimal multivariable individual pitch control for load reduction of large wind turbines is another optimal control technique presented in [45]. An individual pitch controller is designed as a multivariable system to reject the periodic load disturbances optimally. By studying the frequency response of the system rotational speed variations effect the flexible modes of blades. The obtained Multiple Input Multiple Output (MIMO) system is compared with PI-based Individual Pitch Control system using a H-infinity optimization problem. Finally, the dynamic load mitigation of the developed controller is studied through the fatigue load analysis with a high-fidelity aero-elastic simulator. Results show a significant amount

of load alleviation in return for an even lower level of the pitch activity, with respect to the PI-based IPC. IEEE transaction [29] uses an optimal power sharing control of a wind farm where so many Wind Turbines are connected to generate electricity especially in stand-alone farms. There might be lot of supply-demand disturbances when the wind penetration is high, with a proper control design, the power output of a DFIG wind turbine (WT) can be regulated in accordance with the dispatch demand. Specifically, WT can withhold the output power through accelerating its rotor, when there is over-generation. This is often referred to as the deloading control of WT. Similarly, the overloading control can be applied to WT through decelerating its rotor, when there is over-consumption. To implement the overloading and deloading control, the simplest approach is to share the power reference to all he WT in the farm equally. Since, the overloading and deloading capacities of each WT is not equal as they do not have similar wind conditions, a tailor-made control strategy is proposed in this study where power reference of each DFIG WT is obtained through a tailor-made optimization, aiming at maximizing the rotor kinetic energy stored in all WTs within a farm.The above mentioned optimal control methods are the few recent publications and there are many more control techniques combined with optimal control to improve the efficiency which will be discussed later on in this study with more detail.

Robust Control

Robust controller deals with uncertainties and fluctuations in the input to guarantee robust performance of controller under uncertain conditions. The controllers robustness may be designed for frequent fluctuations in the wind speed, to maintain a stable output power from the wind turbine, to maintain the fluctuations in the current or to maintain whatever parameter that needs to put under constant check for the rapid disturbances. The research studies in [17], [19], [40] proposed Robust

control for WECS. Researcher in [17] studied a robust controller for controlling the Pitch angle of the blades of Wind turbine to adapt to the frequent changes in wind speeds for levelling out the converted wind energy into mechanical energy, which is very useful in areas where there is lot of fluctuating wind energy available with wide wind speed region even subject to large parametric or non-parametric disturbances.The study in [19] deals with design of a H robust controller which deals with the selective harmonic filtering in an offshore transmission network subject to parameter perturbations. The authors in [40] evaluated robust control of Variable-speed fixed pitch WECS to evaluate the MPTT with higher precision. [24] deals with a Non-linear robust control to maximize the energy capture in an induction generator based WECS by controlling the tip speed ratio, via the rotor angular speed, to an optimum point at which the efficiency constant (or power coefficient) is maximal for a particular blade pitch angle and wind speed. Even though, the WECS system is a Non-linear model, instead of building a Linear Parameter Varying (LPV) model the authors in [46] considered many operating points and the non-linear model is linearized around these operating points and a robust controller is built for each and every one of these linearized operating points to maximize the energy capture under different wind speeds. Switching among the different H controllers is done by gain-scheduling mechanism using Lagrange interpolation, this method was able to extract maximum energy at the specific speeds of the operating points but, lacked the smooth transition between the discrete bands of speeds of the operating points.

Adaptive Control

Adaptive control is more useful when there is difficulty in constructing the precise model of a Non-linear system which is influenced by the unknown parameters. To cope with the highly nonlinear characteristics of WECS, adaptive control strategies

are very much needed for the complex control systems of WECS. In adaptive control techniques two or more parameters are controlled in a different manner for different situations to optimize the energy conversion.

The different Adaptive control techniques for WECS in [25], [44], [21] are used to achieve different goals for the non-linear WECS. In [25] a Neural-Network (NN) is proposed different operation modes for a VSVP WECS the Torque control at lower speeds, Pitch control at higher speeds and the smooth transition between both the modes of operation The adaptive NN control approximates the nonlinear dynamics of the wind turbine based on input/output measurements and ensures smooth tracking of the optimal tip-speed-ratio at different wind speeds. The robust NN weight updating rules are obtained using Lyapunov stability analysis. The proposed control algorithm is first tested with a simplified mathematical model of a wind turbine, and then the validity of results is verified by simulation studies on a 5 MW wind turbine simulator. [44] illustrates an Adaptive fractional sliding mode control for Double-Fed Induction Generator (DFIG) based WECS,this paper proposes a novel fractional order adaptive terminal sliding mode control system for both the rotor and grid side converters of the DFIG system and stability of the system is of closed-loop system is ensured by the fractional order Lyapunov theorem. The study in [21] presents a Maximum Power Point Tracking (MPPT) using adaptive control for a small scale WECSs to maximize the energy conversion efficiency in a turbulent wind environment. The proposed algorithm uses computational behavior of hill climb search, feedback of tip-speed ratio and power signal for the adaptability over the wind speed range of the WECS and MPPT, the control technique was tested on a WECS emulator to show the improvement in efficiency of this MPPT technique in a gradually fluctuating wind conditions.

Model Predictive Control

Model Predictive Control (MPC) is an appealing control Technique which is of great use in dealing with Non-linear systems with constraints.MPC models predict the change in the dependent variables of the modeled system that will be caused by changes in the independent variables. Model predictive controllers rely on dynamic models of the process, most often linear models obtained by system identification. MPC is universally used as a digital control technique, although there is research into achieving faster response using analog circuitry. It is ,more sensible to use MPC for WECS, if the behaviour of wind has many different particular patterns but not occurring in a specific sequence of patterns, then Model Predictive Controller detects these patterns and matches the model to act accordingly.

The researchers in [52] presented an MPC technique for power tracking and minimizing the mechanical load on wind turbines for the optimal active power control of a wind farm. Instead of linearizing the model at few operating points, the nonlinearities of the wind turbine model are represented by a piece-wise static function based on the wind turbine system inputs and state variables. The nonlinearity identification is based on the clustering-based algorithm, which combines the clustering, linear identification, and pattern recognition techniques. The model used in the study consisted of 47 affine dynamics , is verified by the comparison with a widely used nonlinear wind turbine model. This technique could be used in model prediction of Model Predictive controller or other advanced Optimal control techniques used for the wind farms. Research in [49] uses a two step MPC strategy for improving the power conversion. The proposed configuration uses boost converters and diode inverters as intermediate stages for predict a shift in the model of the system. This technique is aimed at PMSG wind turbines rated in Megawatt ranges.

1.4 Problem Statement

The main goals while designing a WECS is to build a Wind Turbine which is capable of converting wind energy into electric energy with no side effects to the environment and the wildlife surrounding it, we must also consider the feasibility, affordability and, maintenance cost along with profitability. Though all of these are important aspects to be considered while installing WECSs but, this research concerns with the Control issues related to the WECS. The above discussion indicates that there are many different varieties of control techniques. The most important aspect that associated with the control techniques of WECS are as follows:

1. *Conversion Efficiency:* The efficiency of power is improved in the partial load conditions when the wind speeds are below the rated speeds of the WECSs using MPPT, which calculates and controls the generator speed according to the variations in Wind speed. But in full load condition or at wind speeds higher than the rated speeds, the generator rotates at its top rated speed but, not above that to protect the generator power electronic system.

2. *Power Regulation:* The electricity generated by the wind turbine is generated to be used by other electrical devices which have limitations and requirements on power that they can operate under. So, the power that is generated by WECS must be regulated to some standards depending on the requirements, especially when the wind speeds are higher the power generated must be clipped to the rated value of the WECS. To achieve this the common strategy is to change the Pitch angle of the blades to reduce the aerodynamic power captured, which in turn reduces the output power.

3. *Power Quality Control:* To ensure the proper operation and longevity of the

devices that are using the power generated by WECS, good quality of power is needed with limited number of fluctuations within the limits and in some cases must satisfy the standards, of active and reactive power, frequency fluctuation standards, Harmonic noise intensity etc. This issue is handled by the controllers in Power electronic conversion systems.

4. *Robustness:* The performance of the WECS must not deteriorate in case of frequent changes in the wind speeds and it must be able to withstand extreme weather conditions for the feasibility purposes. Robustness is achieved altogether by pitch control, power conversion control techniques and by classifying different operating regions and methods to operate in those regions.

5. *Fatigue Load Reduction:* The fatigue load must always be monitored and controlled in all the kinds of loads. Power maximization is not the goal in all the case which might also maximize the fatigue load and constant presence of such load is very bad for the health and presence of key and costly components which might increase the maintenance cost. Therefore, the trade-off between maximizing captured power and minimizing fatigue loads must necessarily be taken into account by the control system.

1.5 Research Objectives

From the discussion made in Section 1.3 we can deduce some conclusions. Though there have been so many research studies in WECS, there is still a lot of room for improvement as all the different possibilities of control strategies have not been explored. Firstly, most of the reports and studies have considered the mechanical and electrical dynamics separately while modelling the WECS which does not consider

the effect of interaction between the dynamics and specifically using of Time Scales makes it easier to solve such problems and also there have not been many research studies conducted on the usage of time-scales on WECS. Secondly, there have been a lot of studies on linear control of WECS but, non-linear control methods have not been addressed significantly, finally and most importantly there have been very few studies which comprehensively explain the Variable Speed Variable Pitch (VSVP) WECS. From the discussions research objectives have been proposed as follows:

1. *Modelling :* In this research, unlike most works reviewed in Section 1.3, an attempt is made to integrate both mechanical and electrical dynamics in modeling. The developed models represent variable-speed variable pitch WECS with PMSG. The research focuses on both grid-connected and standalone WECS.

2. *Singular perturbation and time scale analysis and synthesis:* Based on the nature of the WECS which contains both slow and fast dynamics, the singular perturbation method is utilized to decouple the overall WECS into slow and fast subsystems. Optimal control techniques Linear Quadratic Regulator (LQR) and Linear Quadratic Gaussian (LQG) are employed to synthesize controllers for both original or decomposed subsystems. Control performances of both original (high-order) and reduced-order controllers are also compared to show the effectiveness of the singular perturbation and time scale methods.

3. *Modelling and Controller design for a VSVP WECS :* Ability to control the pitch angle for WECS gives another degree of freedom which helps in maintaining the output power quality over wide range of wind speeds with little to no Fatigue load on the wind turbine as the force exerted by wind on the turbine can be changed easily by changing the pitch angle of the blades. So the modelling and LQG and LQR controller synthesis are done for the VSVP WECS.

1.6 Overview

This research projects includes 6 chapters and the details of each chapter are as follows:

Chapter 1 begins with some background about wind energy and WECS. The main objective of this chapter is to familiarize readers with WECS by reviewing fundamental knowledge of wind energy developments and wind turbines. The chapter also includes a comprehensive overview of advanced control approaches for WECS, which helps identify control problems of WECS. Specific research directions of the project are discussed in the end of this chapter.

Chapter 2 deals with the dynamic modelling of WECS. In this chapter, system dynamics of WECS from the control view point are addressed and described in forms of mathematical models. Dynamic non-linear model is discussed follwed by linearization process of the model.

Time scales and singular perturbation methods for WECS are addressed in Chapter 3. The chapter begins with the time scale analysis of the modelled VSVP WECS to decompose the original system into slow and fast subsystems.

Chapter 4 then deals with optimal LQR and LQG synthesis for decoupled dynamics in WECS. The singular perturbation method is then proposed for separate slow and fast dynamics existing in WECS to compare the results and, to design optimal LQG controller and filters corresponding to each of the dynamics with the presence of noise and uncertainties.

Chapter 5 explains the results of simulations which implement the theory that has been mentioned in chapters 3 and 4 that have been implemented in MAtlab and Simulink. And finally, chapter 6 concludes the study suggesting some future works.

2 Dynamic modeling of Wind Energy Conversion System

2.1 Introduction

This chapter presents the dynamic modeling of the WECS based upon their physical dynamics. First mathematical representation of WECS derived for different subsystems and then all the subsystems are integrated to obtain the complete nonlinear model for individual representation of complete WECS. The nonlinear model linearization process has also been presented. Part of this chapter is based on the work of [38].

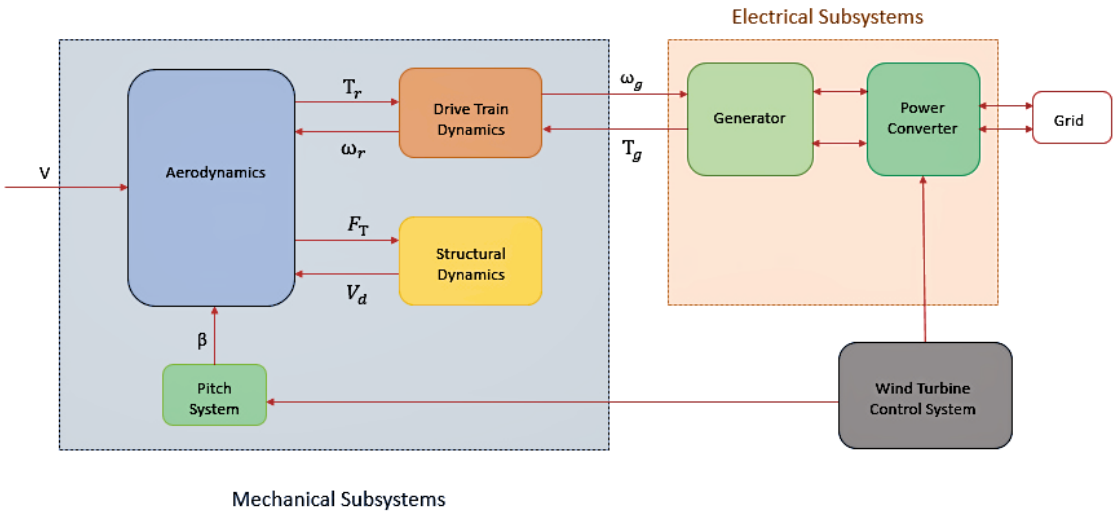

Figure 2.1: WECS Subsystems Modelling and Classification

A model for an entire WECS can be detailed into several interconnected subsystems where as shown in Figure 2.1. WECS consists of different number of devices which are been divided into two groups in terms of dynamics (mechanical and electrical groups) or groups in terms of dynamically represented (drive train dynamics, generator dynamics, aerodynamics, structural dynamics). The model of WECS represent all different types of dynamics. But, for control purposes only, aerodynamics, drive train dynamics and generator dynamics are considered for modelling.

2.2 Aerodynamic Subsystem Modelling

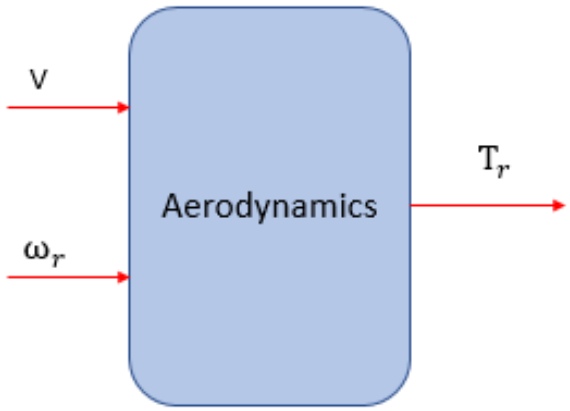

Figure 2.2: Aerodynamic Subsystem

The primary application of wind turbines is to generate energy using the wind. Hence, the aerodynamics is a very important aspect of wind turbines. As wind flows through the wind turbine it exerts force on the blades of the turbine and the force depends on the shape, pitch angle and size of the blades due to which they start

rotating creating aerodynamic torque. There is also force exerted on the tower due to which there is displacement of the tower due to the force (Tower Bending) and also to control the amount of this wind thrust on the blades some of it has to be obstructed by the blades by controlling the pitch angle which causes some undesirable force on the blade leading to blade flapping and bending. The only desirable outcome of this is generation of aerodynamic torque, which ratates the shaft and which in turn rotates the generator to generate the power. To represent the aerodynamic system the Thrust force, Aerodynamic Torque and Mechanical power can be represented as follows:

$$F_T = \frac{1}{2}\rho\pi R^3 C_T(\lambda,\beta)V^2 \tag{2.2.1}$$

$$T_r = \frac{1}{2}\rho\pi R^3 C_Q(\lambda,\beta)V^2 \tag{2.2.2}$$

$$P_m = \frac{1}{2}\rho\pi R^3 C_P(\lambda,\beta)V^3 \tag{2.2.3}$$

where ρ is the air density; V is the wind speed; R is the radius of the wind rotor plane; C_T , C_Q, and C_P are thrust force, torque, and power coefficients, respectively; β is the pitch angle of blades; and λ is the tip-speed ratio which is defined as the ratio between the speed at the tip of blades and the wind speed and can be mathematically expressed as:

$$\lambda = \frac{\omega_r R}{V} \tag{2.2.4}$$

The relationship between the torque coefficient and the power coefficient is defined

as:

$$C_Q = \frac{C_P}{\lambda} \tag{2.2.5}$$

The power coefficient has been approximated from [32, 31] as:

$$C_P(\lambda, \beta) = C_1(\frac{C_2}{\lambda_i} - C_3\beta - C_4)exp(\frac{-C_5}{\lambda_i}) + C_6\lambda \tag{2.2.6}$$

where:

$$\lambda_i = \frac{1}{\frac{1}{\lambda + C_7\beta} - \frac{C_8}{1+\beta^3}} \tag{2.2.7}$$

or from [1, 2, 33] as:

$$C_P(\lambda, \beta) = (C_9 - C_{10}\beta)sin(\frac{\pi(\lambda + C_{11})}{C_{12} - C13\beta}) - C_{14}(\lambda - 3)\beta \tag{2.2.8}$$

The aerodynamic subsystem block as shown in Figure 2.2 takes the wind speed V and the wind rotor rotational speed ω_r as the inputs and gives the aerodynamic torque T_r as the output.

2.3 Drive Train Subsystem Modelling

The Drive train Subsystem transmits and increases the rotational speed from the turbine rotor to generator of the turbine, it is also used for braking the speed of the wind turbine rotor to keep it in the limits of generator rotational speeds. Breaking mechanism is more related to mechanical engineering perspective than the control perspective so in this section modelling of drive train mechanism is taken care of. The drive train subsystem takes aerodynamic torque τ_r and generator torque as inputs

and the angular velocity of rotor ω_r and angular velocity of generator ω_g as outputs as shown in Figure 2.3. The drive train connects the wind rotor shaft (low speed shaft) to the generator shaft (high speed shaft) through a gear box, which can be represented by a speed multiplier $1/i$ with an efficiency η.

Figure 2.3: Drive Train Subsystem

2.3.1 Drive Train Dynamics

The dynamics for drive train deals with transmission of torque from low speed shaft to high speed shaft connected to generator rotor. The derivation of dynamics of the drive train are as follows:

Differential equation of low speed shaft is

$$J_r\dot{\omega}_r = T_r - \frac{i}{\eta}T_H \tag{2.3.1}$$

Where J_r is the wind rotor inertia, ω_r is the wind rotor angular velocity,and T_r is the aerodynamic torque and T_H is the internal torque.

As the torque is not transmitted completely as there will be losses and also there is some energy stored in form of momentum of the shaft to compensate for all the

measures high speed shaft is considered as a flexible and that is represented by adding a spring to the high speed shaft. So the derivations of the high speed shaft side are

$$J_g\dot{\omega_g} = T_H - T_g, \tag{2.3.2}$$

$$\dot{T_H} = K_g(\omega_H - \omega_g) + B_g(\dot{\omega_H} - \dot{\omega_g}). \tag{2.3.3}$$

where J_g is the generator inertia, T_g is the generator electromagnetic torque, ω_H is the smaller gear speed, ω_g is the generator speed, K_g and B_g are the stiffness and damping coefficients of the high-speed shaft, respectively. Replacing $\omega_H = i\omega_r$ into (2.3.3) gives

$$\dot{T_H} = K_g(i\omega_r - \omega_g) + B_g(i\dot{\omega_r} - \dot{\omega_g}). \tag{2.3.4}$$

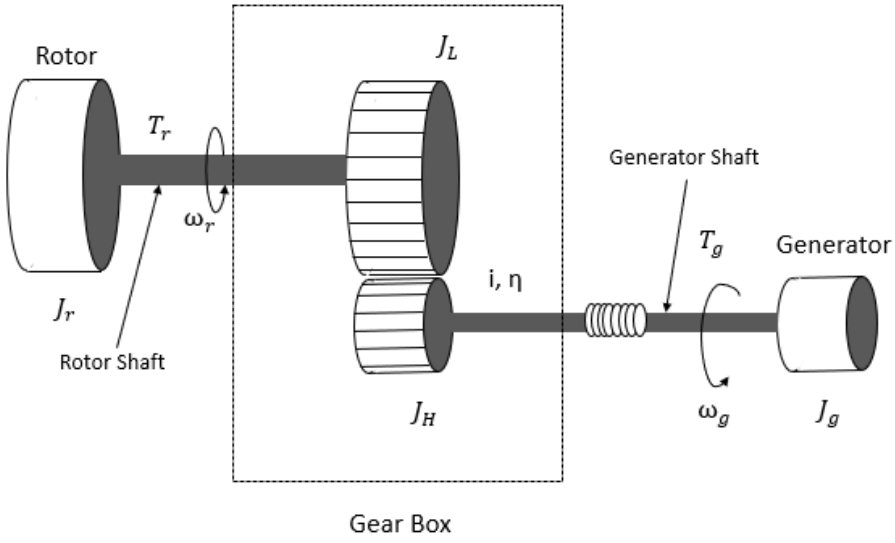

Figure 2.4: Drive Train Diagram

Combining (2.3.1), (2.3.2) and (2.3.4) gives the drive train model as:

$$\dot{\omega_r} = -\frac{i}{\eta J_r} T_H + \frac{1}{J_r} T_r, \tag{2.3.5}$$

$$\dot{\omega_g} = \frac{1}{J_g} T_H - \frac{1}{J_g} T_g, \tag{2.3.6}$$

$$\dot{T_H} = iK_g\omega_r - K_g\omega_g - Bg(\frac{1}{J_g} + \frac{i^2}{\eta J_r})T_H + \frac{iB_g}{J_r}T_r + \frac{B_g}{J_g}T_g \tag{2.3.7}$$

2.4 Generator Modelling

Permanent Magnet Synchronous Generator (PMSG) is the most widely used generator in WECS. So in this section dynamics of a Grid connected PMSG are modelled. PMSG is an electrical component so, it can be represented by an electrical circuit diagram which is shown in the diagram below.

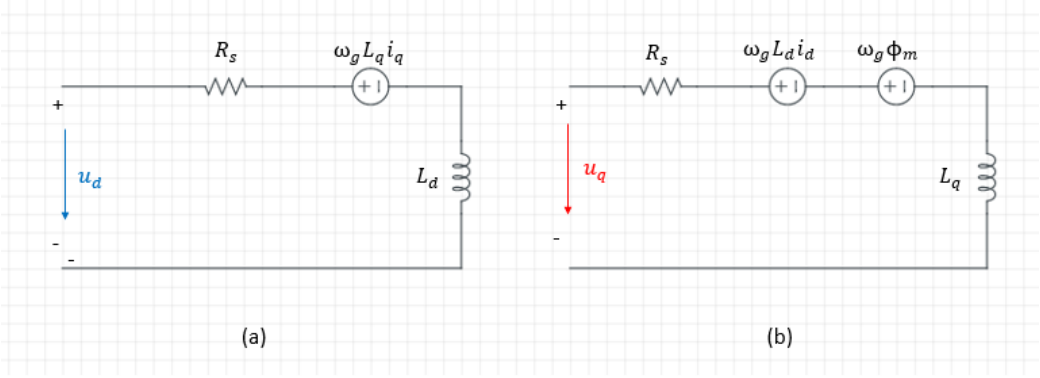

Figure 2.5: PMSG equivalent circuit diagram. (a) d-axis equivalent (b) q-axis equivalent

The circuit diagram representation of the Grid connected PMSG is shown in the diagram Fig 2.5 above and the mathematical representation can be derived for the

(d,q) axes from these circuit diagrams as follows:

$$u_d = -R_s i_d + L_q i_q \omega_s - L_d \dot{i_d}, \tag{2.4.1}$$

$$u_q = -R_s i_q - L_q \dot{i_q} - (L_d i_d - \phi_m)\omega_s \tag{2.4.2}$$

where R_s is the stator winding resistance and L_d and L_q are d and q components of the stator inductance, respectively; u_d and i_d are the d component voltage and current of the stator, u_q and i_q are the q component voltage and current of the stator respectively; and ϕ_m is the flux linkage of the stator winding and $\omega_s = p\omega_s$ is the stator angular frequency (where p is the number of poles pairs used in the PMSG). The generator electromagnetic torque can be derived as:

$$T_g = p\phi_m i_q \tag{2.4.3}$$

By rearranging the equations (2.4.1) and (2.4.2) the dynamic equations of the grid connected PMSG are as follows:

$$\dot{i_d} = -\frac{R_s}{L_d} i_d + \frac{pL_q}{L_d} i_q \omega_g - \frac{1}{L_d} u_d, \tag{2.4.4}$$

$$\dot{i_q} = -\frac{R_s}{L_q} i_q + \frac{p}{L_q}(L_d i_d - \phi_m)\omega_g - \frac{1}{L_q} u_q \tag{2.4.5}$$

2.5 Pitch Subsystem Modelling

The actuator consisted of counter weights that enable the rotation of the blades around their longitudinal axes. As turbine size increased, these rudimentary mechanisms were replaced by hydraulic or electro mechanical devices. The higher exibility of these devices permitted the implementation of ecient and reliable control strategies for power or speed limitation. The pitch actuator is a nonlinear servo motor that generally rotates all the blades or part of them in unison.

The pitch subsystem takes the input from the control system which decides the angle of the blades (desired pitch angle) β_d at different wind speed and at different power requirements to optimize the output power and the output is the final pitch angle of the blades β.

Figure 2.6: Pitch System

The pitch actuator system can be modelled as a first-order system with saturation in the amplitude and derivative β as [42, 14]

$$\dot{\beta} = -\frac{1}{\tau}\beta + \frac{1}{\tau}\beta_d \tag{2.5.1}$$

where,

$$\beta_{min} \leq \beta \leq \beta_{max}, \tag{2.5.2}$$

$$\dot{\beta}_{min} \leq \dot{\beta} \leq \dot{\beta}_{max} \tag{2.5.3}$$

Here τ is the time constant of the pitch system and variables with min and max suffixes are the respective minimum and maximum values for that corresponding variable.

2.6 Non-linear Model of the Entire WECS

Whole WECS can be represented different subsystems interacting together to convert the wind energy into electrical energy and these non-linear dynamic model can be explained by the equations which show the way in which the conversion is done and control that conversion in a desired manner to get the required output.

The Grid-connected flexible drive train PMSG WECS can be represented by combining (2.2.2), (2.3.5), (2.3.6), (2.3.7),(2.4.3), (2.4.4), (2.4.5) and (2.5.1) which gives:

$$\dot{\omega_r} = -\frac{i}{\eta J_r} T_H + \frac{1}{2J_r} \rho \pi R^3 C_Q(\lambda, \beta) V^2, \tag{2.6.1}$$

$$\dot{\omega_g} = \frac{1}{J_g} T_H - \frac{1}{J_g} p \phi_m i_q, \tag{2.6.2}$$

$$\dot{T_H} = iK_g\omega_r - K_g\omega_g - Bg(\frac{1}{J_g} + \frac{i^2}{\eta J_r})T_H + \frac{iB_g}{2J_r}\rho\pi R^3 C_Q(\lambda, \beta)V^2 + \frac{B_g}{J_g} p\phi_m i_q, \tag{2.6.3}$$

$$\dot{i_d} = -\frac{R_s}{L_d} i_d + \frac{pL_q}{L_d} i_q \omega_g - \frac{1}{L_d} u_d, \tag{2.6.4}$$

$$\dot{i_q} = -\frac{R_s}{L_q} i_q + \frac{p}{L_q} (L_d i_d - \phi_m) \omega_g - \frac{1}{L_q} u_q \tag{2.6.5}$$

$$\dot{\beta} = -\frac{1}{\tau} \beta + \frac{1}{\tau} \beta_d \tag{2.6.6}$$

Where λ and $C_Q(\lambda, \beta)$ are defined by (2.2.4), (2.2.5) and (2.2.6).

2.7 Linearized Model

For linearizing the above non-linear model at an operating point, the non-linearity is because of the turbine torque (T_r) which is an element of few equations, so linearization of turbine torque at an operating point can be done as follows:

$$\delta T_r = L_\omega(\bar{\omega_r}, \bar{v}, \bar{\beta}) \delta\omega_r + L_v(\bar{\omega_r}, \bar{v}, \bar{\beta}) \delta v + L_\beta(\bar{\omega_r}, \bar{v}, \bar{\beta}) \delta\beta \tag{2.7.1}$$

$$L_\omega(\bar{\omega_r}, \bar{v}, \bar{\beta}) = \frac{\partial T_r}{\partial \omega_r}|_{(\bar{\omega_r}, \bar{v}, \bar{\beta})} \tag{2.7.2}$$

$$L_v(\bar{\omega_r}, \bar{v}, \bar{\beta}) = \frac{\partial T_r}{\partial v}|_{(\bar{\omega_r}, \bar{v}, \bar{\beta})} \tag{2.7.3}$$

$$L_\beta(\bar{\omega_r}, \bar{v}, \bar{\beta}) = \frac{\partial T_r}{\partial \beta}|_{(\bar{\omega_r}, \bar{v}, \bar{\beta})} \tag{2.7.4}$$

where δ represents the derivative of the variable at the operating point, whereas over bar of a variable (i.e: $\bar{\omega}$) represents variable value at the operating point.

The state vectors is $X = [x_1, x_2, x_3, x_4, x_5, x_6]^T = [\omega_r, \omega_g, T_H, \beta, i_d, i_q]^T$ and the control vector is $u = [u_1, u_2, u_3, u_4]^T = [u_d, u_q, V, \beta_d]^T$. Choosing the operating point with $\bar{X} = [\bar{\omega_r}, \bar{\omega_g}, \bar{T_H}, \bar{i_d}, \bar{i_q}, \bar{\beta}]^T$ and $\bar{u} = [\bar{u_d}, \bar{u_q}, \bar{V}, \bar{\beta_d}]^T$. So the linearized system and control matrices at the operating point are given as:

$$A(\bar{x}, \bar{u}) = \begin{bmatrix} \frac{L_\omega}{J_r} & 0 & \frac{-i}{\eta J_r} & \frac{L_\beta}{J_r} & 0 & 0 & \\ 0 & 0 & \frac{1}{J_g} & & 0 & 0 & \frac{-p\phi_m}{J_g} \\ iK_g + \frac{iB_g}{J_r}L_\omega & -K_g & -B_g(\frac{1}{J_g} + \frac{i^2}{\eta J_g}) & \frac{iB_g}{J_r}L_\beta & 0 & \frac{B_g p\phi_m}{J_g} & \\ 0 & 0 & 0 & -\frac{1}{\tau} & 0 & 0 & \\ 0 & \frac{pL_q}{L_d}\bar{i_q} & 0 & 0 & -\frac{R_s}{L_d} & \frac{pL_q}{L_d}\bar{\omega_g} & \\ 0 & \frac{-p}{L_q}(L_d\bar{i_d} - \phi_m) & 0 & 0 & -\frac{pL_d\bar{\omega_g}}{L_q} & -\frac{R_s}{L_d} & \end{bmatrix} \tag{2.7.5}$$

$$B(\bar{x}, \bar{u}) = \begin{bmatrix} 0 & 0 & \frac{L_v}{J_r} & 0 \\ 0 & 0 & 0 & 0 \\ 0 & 0 & \frac{iB_g}{J_r}L_v & 0 \\ 0 & 0 & 0 & \frac{1}{\tau} \\ -\frac{1}{L_d} & 0 & 0 & 0 \\ 0 & -\frac{1}{L_q} & 0 & 0 \end{bmatrix} \tag{2.7.6}$$

2.8 Chapter Summary

In this chapter, mathematical representation of all the different subsystems have been modelled and presented. The modelling of the sub-systems related the control systems only have been presented in this chapter. The focus was on PMSG based grid-connected WECS, first the non-linear dynamics have been presented and then a a procedure to obtain the state-space vectors of the linearized model at a specific operating point has been presented, which is required to apply the singular perturbation and time-scales method which is presented in Chapter 3.

3 Singular Perturbation and Time Scales Analysis and Synthesis

3.1 Introduction

One of the most important objective while designing a controller is to obtain optimal energy conversion rate under all the different wind conditions, most commonly traditional MPPT control strategy is used to achieve this goal but, it generates a fatigue load on the tower. So, an optimal control strategy which can optimize the energy conversion efficiency and reduce the fatigue load on the tower has been introduced to WECS. However, such optimal controller design for WECS results in high-order controllers which are more expensive and complex to implement. Based on this limitation, authors in [23] have proposed an idea of designing separate controllers for the two time-scales but, it does not provide complete decoupling of the dynamics of two different time scales leading to reduction of performance of the controllers. This problem has been solved in this research study for the VSVP WECS by using the singular perturbation and time scale methods, providing an effective means of decoupling slow and fast dynamics in WECS completely. After the dynamics are decoupled independant optimal controllers are designed for both slow and fast dynamics separately.

In this chapter application of Singular perturbation and time scales on VSVP

WECS is explained in detail. By applying time-scales the linearized system is decomposed into reduced-order independent slow and fast sub-systems. Synthesis and simulation of different independent optimal-controlers for both slow and fast subsystems is done like: Linear Quadratic Guassian (LQG) and Linear Quadratic REgulator (LQR) are investigated combining the techniques used in other systems in [37, 51].

3.2 Time Scales Derivation

To decouple the slow and fast sub-systems from the higher-order system the following procedure is used if is a singularly perturbed system. To know more about the properties and behaviour of singularly perturbed systems refer to [35, 34].

3.2.1 Block Diagonalization Technique

A linear Singularly perturbed continuos system can be expressed in the form:

$$\dot{X_1} = A_1 X_1 + A_2 X_2 + B_1 u, \tag{3.2.1}$$

$$\epsilon \dot{X_2} = A_3 X_1 + A_4 X_2 + B_2 u \tag{3.2.2}$$

where X_1 and X_2 are $mandn$ dimensional slow and fast state-vectors, respectively and u is an r dimensional control vector and $X_{1-4} and B_{1-2}$ are time-invariant matrices with appropriate dimensions and ϵ is a very small positive parameter which parameterizes singular pertuburated form.

Chang's transform [6] is a technique used to decompose the system into slow and fast subsystems. The transformation has two steps as follows:

Step I: Choosing a new variable X_f where:

$$X_f = X_2 + LX_1 \tag{3.2.3}$$

or

$$X_2 = X_f - LX_1 \tag{3.2.4}$$

where L is a matrix of appropriate dimensions and multiplying ϵ on both sides and differentiating the equation (3.2.3) gives:

$$\begin{aligned} \epsilon\dot{X_f} &= \dot{X_2} + \epsilon L\dot{X_1} \\ &= (A_3 + \epsilon LA_1)X_1 + (A_4 + \epsilon LA_2)X_2 + (B_2 + \epsilon LB_1) \end{aligned} \tag{3.2.5}$$

Substituting (3.2.4) in (3.2.5) gives:

$$\epsilon\dot{X_f} = (A_3 + \epsilon LA_1 - A_4L - \epsilon LA_2L)X_1 + (A_4 + \epsilon LA_2)X_f + (B_2 + \epsilon LB_1)u \tag{3.2.6}$$

Choosing L such that

$$A_3 + \epsilon LA_1 - A_4L - \epsilon LA_2L = 0 \tag{3.2.7}$$

Then equation (3.2.6) becomes:

$$\epsilon\dot{X_f} = (A_4 + \epsilon LA_2)X_f + (B_2 + \epsilon LB_1)u \tag{3.2.8}$$

Substituting (3.2.4) into (3.2.1) gives:

$$\dot{X_1} = (A_1 - A_2L)X_1 + A_2X_f + B_1u \tag{3.2.9}$$

Combining equations (3.2.8) and (3.2.9) transforms the system (3.2.1) and (3.2.2) into:

$$\begin{bmatrix} \dot{x_1} \\ \epsilon \dot{x_f} \end{bmatrix} = \begin{bmatrix} A_s & A_2 \\ 0 & A_f \end{bmatrix} \begin{bmatrix} x_1 \\ x_f \end{bmatrix} + \begin{bmatrix} B_1 \\ B_f \end{bmatrix} u \tag{3.2.10}$$

where

$$A_s = A_1 - A_2 L, \tag{3.2.11}$$

$$A_f = A_4 + \epsilon L A_2, \tag{3.2.12}$$

$$B_f = B_2 + \epsilon L B_1. \tag{3.2.13}$$

Step II: Choosing another new variable X_s where:

$$X_s = X_1 - H X_f \tag{3.2.14}$$

or

$$X_1 = X_s + H X_f \tag{3.2.15}$$

where H is a a matrix with appropriate dimensions. Differentiating equation (3.2.14) on both sides gives:

$$\begin{aligned} \epsilon \dot{X}_s &= \dot{X}_1 - H \dot{X}_f \\ &= A_s X_s + (A_s H + A_2 - \frac{1}{\epsilon} H A_f) X_f + (B_1 - \frac{1}{\epsilon} H B_f) u \end{aligned} \tag{3.2.16}$$

Choosing H such that

$$A_s H + A_2 - \frac{1}{\epsilon} H A_f = 0, \tag{3.2.17}$$

or

$$HA_4 - A_2 + \epsilon(HLA_2 - A_1H + A_2LH) = 0. \tag{3.2.18}$$

Equation (3.2.16) becomes:

$$\epsilon\dot{X}_s = A_sX_s + B_su \tag{3.2.19}$$

where

$$\begin{aligned} B_s &= B_1 - \frac{1}{\epsilon}HB_f, \\ &= B_1 - \frac{1}{\epsilon}HB_2 - \epsilon HLB_1. \end{aligned} \tag{3.2.20}$$

combining equation (3.2.8) and (3.2.19) gives two decoupled subsystems as follows:

$$\begin{aligned} \dot{X}_S &= A_sX_s + B_su \\ \epsilon\dot{X}_f &= A_fX_f + B_fu, \end{aligned} \tag{3.2.21}$$

or

$$\begin{aligned} \dot{X}_S &= A_sX_s + B_su \\ \dot{X}_f &= \bar{A}_fX_f + \bar{B}_fu \end{aligned} \tag{3.2.22}$$

where

$$\bar{A_f} = \frac{1}{\epsilon}A_f, \tag{3.2.23}$$

$$\bar{B_f} = \frac{1}{\epsilon}B_f. \tag{3.2.24}$$

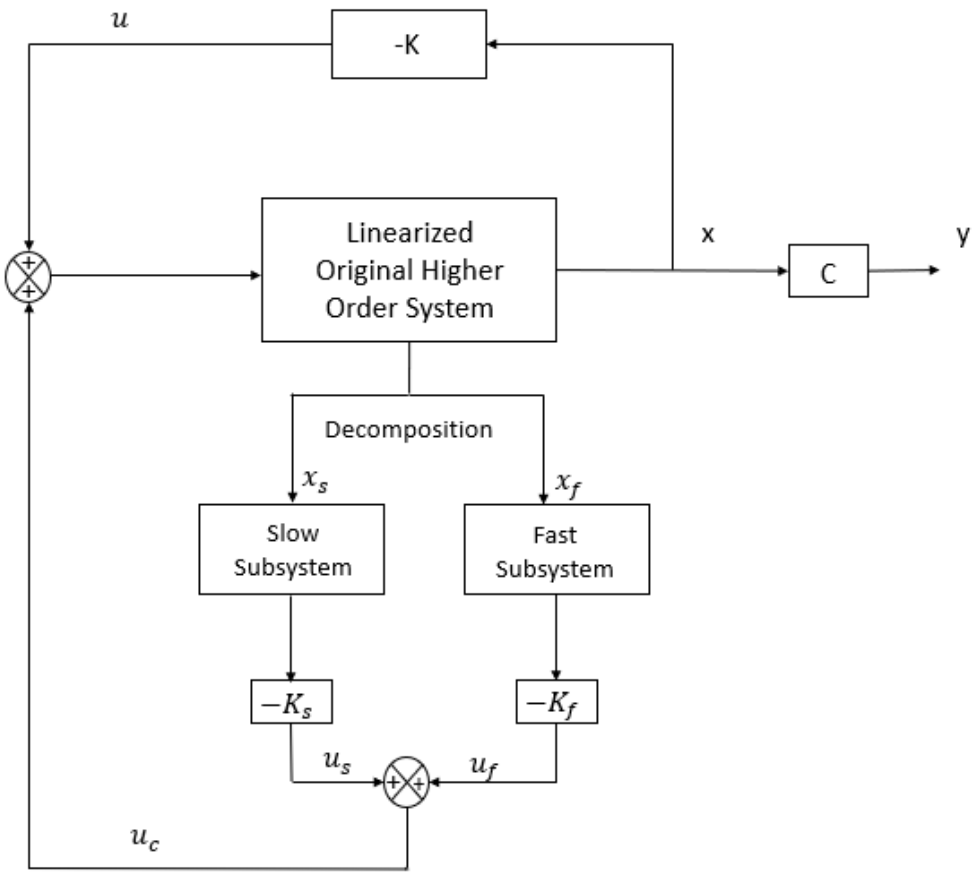

Figure 3.1: Time Scale LQR control diagram

Once the two time scales have been decoupled from the original system using the above derivation as shown in (3.2.21), the controller of each sub-system can be designed individually as shown in Figure 3.1.

The system in equations (3.2.1) and (3.2.2) can be represented in the state space representation as follows:

$$\begin{bmatrix} \dot{x_1} \\ \epsilon\dot{x_2} \end{bmatrix} = \begin{bmatrix} A_1 & A_2 \\ \frac{1}{\epsilon}A_3 & \frac{1}{\epsilon}A_4 \end{bmatrix} \begin{bmatrix} x_1 \\ x_2 \end{bmatrix} + \begin{bmatrix} B_1 \\ \frac{1}{\epsilon}B_2 \end{bmatrix} u \tag{3.2.25}$$

Any linear system can be written in the form of (3.2.25) with parameter ϵ. In this case, we need to estimate the value of ϵ from the system. One way to estimate ϵ is by computing the ratio between the largest absolute eigenvalue of the slow subsystem state space matrix and the smallest absolute eigenvalue of the fast subsystem state space matrix [35]. In addition, it is required to arrange states as a group of slow states (x_s) and a group of fast states (x_f) by a linear transformation called permutation. For more details of permutation, readers are referred to [35].

3.2.2 Recursive Algorithms

To get any system into the form shown above in (3.2.25) procedure requires solutions of non-symmetric Riccati-type matrix equations (3.2.7) and (3.2.17). And there are two algorithms to solve such equations:

1. Fixed Point Algorithm [16, 35, 26]
2. Newton Algorithm [16, 18]

Fixed Point Algorithm

This algoritm converges at the rate of $O(\epsilon)$, under the condition that A_4 is non-singular matrix. The solutions of L and H can be obtained by following method:

$$A_4 L(k+1) = A_3 + \epsilon L(k)[A_1 - A_2 L(k)], \tag{3.2.26}$$

$$H(k+1)A_4 = A_2 - \epsilon[H(k)L(k)A_2 - A_1 H(k) + A_2 L(k)H(k)] \tag{3.2.27}$$

with $k = 1, 2, 3...$ where,

$$L(0) = A_4^{-1} A_3, \tag{3.2.28}$$

$$H(0) = A_2 A_4^{-1} \tag{3.2.29}$$

Fixed point algorithm converges only if the following condition holds:

$$||A_4^{-1}|| \leq \frac{1}{3}(||A_0|| + ||A_2||||L_0||)^{-1} \tag{3.2.30}$$

where

$$A_0 = A_1 - A_2 L_0 \tag{3.2.31}$$

Newton Algorithm

Newton algorithm converges at the rate $O(\epsilon^{2^k})$ which is faster than fixed point algorithm with the condition A_4 is a nonsingular matrix. And the solution for L can be obtained by following procedure:

$$D_1(k)L(k+1) + L(k+1)D_2(k) = Q(k), \tag{3.2.32}$$

where

$$D_1(k) = A_4 + \epsilon L(k) A_2, \tag{3.2.33}$$

$$D_2(k) = -\epsilon[A_1 - A_2 L(k)], \tag{3.2.34}$$

$$Q(k) = A_3 + \epsilon L(k) A_2 L(k) \tag{3.2.35}$$

where

$$L(0) = A_4^{-1} A_3 \tag{3.2.36}$$

After solving for L, the solution for H can be obtained by solving the Sylvester equation:

$$H(k+1)D_1(k+1) + D_2(k+1)H(k+1) = A_2. \tag{3.2.37}$$

where:

$$H(0) = A_2 A_4^{-1} \tag{3.2.38}$$

The sufficient condition for convergence of the Newton algorithm is:

$$||\Delta L_k|| \leq ||Q_K|| = ||A_3 + \epsilon L_k A_2 L_k|| \tag{3.2.39}$$

3.3 Time Scale Analysis of a Grid-Connected PMSG Based WECS

In this section Grid-connected PMSG is decoupled into slow and fast subsystems, whose parameters are listed in table 3.1 below,is linearized at an operating point where the maximum aerodynamic torque (i.e. maximum power) corresponding to each wind speed and pitch angle is reached; thus a different wind speed and pitch angle induces different linear model and corresponding controller. In real time the control system switches among the different pre-designed controllers when ever the speed and pitch angle change. In this research the interest is of designing a controller at one speed and pitch angle. For wind speed $V = 10m/sec$ and pitch angle $\beta = 45/\pi$

, the optimal operating point is:

$$\left\{\begin{array}{l} \bar{\omega_r} = 24.5416 rad/sec, \\ \bar{\omega_g} = 147.2436 rad/sec, \\ \bar{T_H} = 29.0671 N.m, \\ \bar{i_d} = 4.4533 A, \\ \bar{i_q} = 3.5047 A, \\ \bar{\beta_0} = \frac{45}{\pi} \end{array}\right\} = \text{Operating Point} \tag{3.3.1}$$

The value of partial derivatives $L_\omega, L_v and L_\beta$ specified in equations (2.7.2), (2.7.3) and (2.7.4) at the above mentioned operating point are as follows:

$L_\omega = -4.0757$

$L_v = 29.0589$

$L_\beta = -5.6658$

The table below has all the specifications of the Grid-connected PMSG based WECS parameters:

Notation	Description	Values
ρ	Air Density	$1.25 kg/m^3$
R	Blade Length or Wind rotor plane radius	$2.5m$
i	Gear box ratio	6
η	Gear box efficiency	1
J_r	Wind Rotor Inertia	$2.88 kg/m^2$
J_g	Generator Inertia	$0.22 kg/m^2$
K_g	High speed shaft stiffness coefficient	$75 N.m/Rad$
B_g	High speed shaft damping coefficient	$0.3 kg.m^2/s$
p	Number of pole pairs in gennerator	3
R_s	PMSG stator Resistance	3.3Ω
ϕ_m	PMSG flux linkage	$0.4382 Wb$
L_d	PMSG stator d-axis inductance	$41.56 mH$
L_q	PMSG stator q-axis inductance	$41.56 mH$

Table 3.1: Grid-connected PMSG based WECS

So the linearized model of Grid-connected PMSG model after substituting all the values of parameters into the matrices specified in equations (2.7.5) and (2.7.6) and the partial derivatives needed at the specific operating point is as follows:

$$\begin{bmatrix} \dot{\delta_{\omega_r}} \\ \dot{\delta_{\omega_g}} \\ \dot{\delta_{T_H}} \\ \dot{\delta_{\beta}} \\ \dot{\delta_{i_d}} \\ \dot{\delta_{i_q}} \end{bmatrix} = \begin{bmatrix} -1.4152 & 0 & -2.0833 & -1.9673 & 0 & 0 \\ 0 & 0 & 4.5455 & 0 & 0 & -5.9755 \\ 447.4527 & -75 & -5.1136 & -3.5411 & 0 & 1.7926 \\ 0 & 0 & 0 & -10 & 0 & 0 \\ 0 & 10.5141 & 0 & 0 & -79.4032 & 441.7308 \\ 0 & 18.2714 & 0 & 0 & -441.7308 & -79.4033 \end{bmatrix} \begin{bmatrix} \delta_{\omega_r} \\ \delta_{\omega_g} \\ \delta_{T_H} \\ \delta_{\beta} \\ \delta_{i_d} \\ \delta_{i_q} \end{bmatrix} + \begin{bmatrix} 0 & 0 & 10.0899 & 0 \\ 0 & 0 & 0 & 0 \\ 0 & 0 & 18.1618 & 0 \\ 0 & 0 & 0 & 10 \\ -24.0616 & 0 & 0 & 0 \\ 0 & -24.0616 & 0 & 0 \end{bmatrix} \begin{bmatrix} \delta_{u_d} \\ \delta_{u_q} \\ \delta_V \\ \delta_{\beta_d} \end{bmatrix} \tag{3.3.2}$$

The above equation is of the form:

$$\dot{X} = AX + Bu \tag{3.3.3}$$

Because wind is considered as an uncontrollable input all the elements associated with the input variable V in the matrix B are zeroed to isolate the effect of wind

uncontrollability. So, the above equation becomes:

$$\begin{bmatrix} \dot{\delta_{\omega_r}} \\ \dot{\delta_{\omega_g}} \\ \dot{\delta_{T_H}} \\ \dot{\delta_{\beta}} \\ \dot{\delta_{i_d}} \\ \dot{\delta_{i_q}} \end{bmatrix} = \begin{bmatrix} -1.4152 & 0 & -2.0833 & -1.9673 & 0 & 0 \\ 0 & 0 & 4.5455 & 0 & 0 & -5.9755 \\ 447.4527 & -75 & -5.1136 & -3.5411 & 0 & 1.7926 \\ 0 & 0 & 0 & -10 & 0 & 0 \\ 0 & 10.5141 & 0 & 0 & -79.4032 & 441.7308 \\ 0 & 18.2714 & 0 & 0 & -441.7308 & -79.4033 \end{bmatrix} \begin{bmatrix} \delta_{\omega_r} \\ \delta_{\omega_g} \\ \delta_{T_H} \\ \delta_{\beta} \\ \delta_{i_d} \\ \delta_{i_q} \end{bmatrix}$$
$$+ \begin{bmatrix} 0 & 0 & 0 & 0 \\ 0 & 0 & 0 & 0 \\ 0 & 0 & 0 & 0 \\ 0 & 0 & 0 & 10 \\ -24.0616 & 0 & 0 & 0 \\ 0 & -24.0616 & 0 & 0 \end{bmatrix} \begin{bmatrix} \delta_{u_d} \\ \delta_{u_q} \\ \delta_V \\ \delta_{\beta_d} \end{bmatrix} \tag{3.3.4}$$

The representation of the PMSG based WECS in the state space equation above has 6 different state variables with four mechanical state variables (i.e. slow states) wind rotor rotational speed (ω_r), generator rotational speed (ω_g), and internal torque (T_H) and pitch angle (β) along with two electrical state variables (i.e. fast states) the d and q components of the generator current, i_d and i_q. The eigen values of the matrix

A are as follows:

$$\left\{\begin{array}{l} p_1 = -3.58079331042100 + J35.5485392840279, \\ p_2 = -3.58079331042100 - j35.5485392840279, \\ p_3 = -0.685511507233029, \\ p_4 = -10, \\ p_5 = -79.4510343491174 + j441.863044182623, \\ p_6 = -79.4510343491174 - j441.863044182623 \end{array}\right\} = \text{Eigen Values} \qquad (3.3.5)$$

So the poles p_1 to p_4 have smaller magnitude compared to the value to that of p_5 and p_6, so we can divide the sub-systems in the same manner. As shown in the diagram

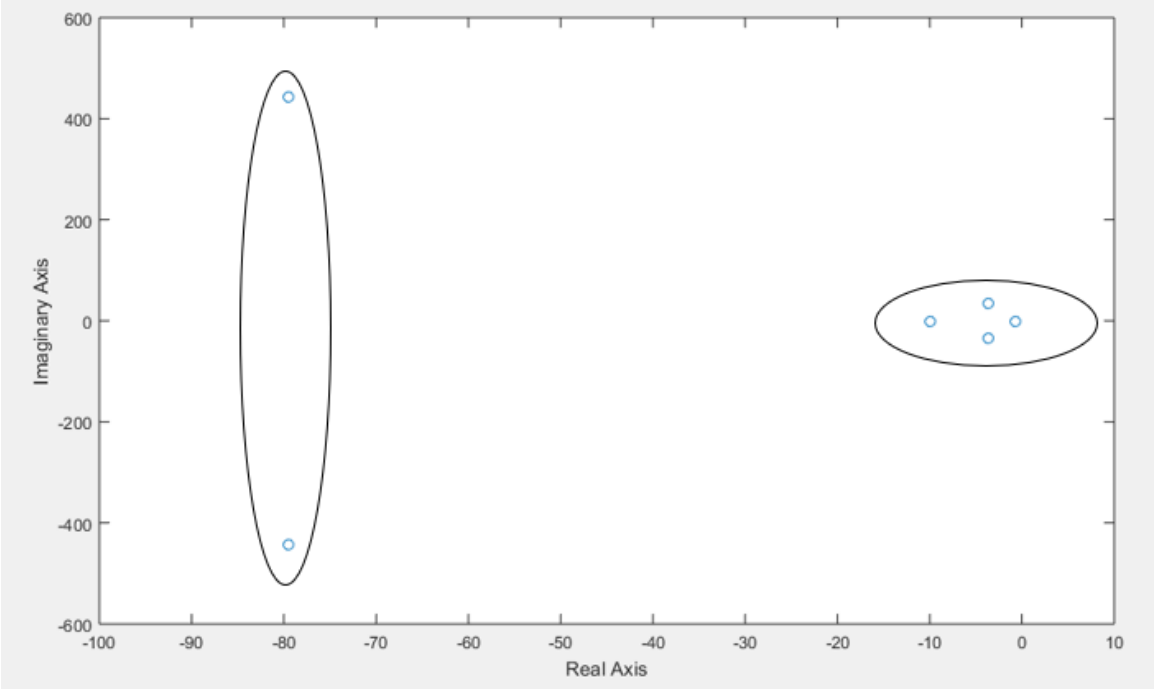

Figure 3.2: Eigen Values Plot

above the two groups of eigen value are far apart so it can be accepted that the system (3.3.4) clearly has time-scales property. For a non-linear PMSG WECS, the

parameter ϵ is determined by the L_q or L_d, the inductance of d and q components of the generator.

The Newton's algorithm and Fixed point algorithm were applied for the system (3.3.4) with value of $\epsilon = 0.04156$ to solve the equation (3.2.7) and (3.2.18). The Newton's algorithm was convergent and at a faster rate and the solution for the equations are as follows:

$$L = \begin{bmatrix} 0 & -0.044 & 0 & 0 \\ 0 & 0.0159 & 0 & 0 \end{bmatrix}, H = \begin{bmatrix} 0 & 0 \\ -13103.95 & 2355.49 \\ 3931.18 & -706.65 \\ 0 & 0 \end{bmatrix} \tag{3.3.6}$$

The subsystem matrices are as follows:

$$\begin{aligned} A_1 &= \begin{bmatrix} -1.41 & 0 & -2.08 & -1.97 \\ 0 & 0 & 4.54 & 0 \\ 447.45 & -75 & -5.11 & -3.54 \\ 0 & 0 & 0 & -10 \end{bmatrix}, A_2 = \begin{bmatrix} 0 & 0 \\ 0 & -5.98 \\ 0 & 1.79 \\ 0 & 0 \end{bmatrix}, \\ A_3 &= \begin{bmatrix} 0 & 10.51 & 0 & 0 \\ 0 & 18.27 & 0 & 0 \end{bmatrix}, A_4 = \begin{bmatrix} -79.40 & 441.73 \\ -441.73 & -79.40 \end{bmatrix}, \\ B_1 &= \begin{bmatrix} 0 & 0 & 0 & 0 \\ 0 & 0 & 0 & 0 \\ 0 & 0 & 0 & 0 \\ 0 & 0 & 0 & 10 \end{bmatrix}, B_2 = \begin{bmatrix} -24.06 & 0 & 0 & 0 \\ 0 & -24.06 & 0 & 0 \end{bmatrix} \end{aligned} \tag{3.3.7}$$

By using the above results and the value of ϵ in the chang's transformation the system in (3.3.4) can be decomposed into slow and fast sub-systems as follows:

Slow Sub-system:

$$\begin{bmatrix} \dot{\delta_{\omega_r}} \\ \dot{\delta_{\omega_g}} \\ \dot{\delta_{T_H}} \\ \dot{\delta_{\beta}} \end{bmatrix} = \begin{bmatrix} -1.41 & 0 & -2.08 & -1.97 \\ 0 & 0.094 & 4.54 & 0 \\ 447.45 & -75.03 & -5.11 & -3.54 \\ 0 & 0 & 0 & -10 \end{bmatrix} \begin{bmatrix} \delta_{\omega_r} \\ \delta_{\omega_g} \\ \delta_{T_H} \\ \delta_{\beta} \end{bmatrix} + \begin{bmatrix} 0 & 0 & 0 & 0 \\ -315302.07 & 56677.09 & 0 & 0 \\ 94590.62 & -17003.13 & 0 & 0 \\ 0 & 0 & 0 & 10 \end{bmatrix} \begin{bmatrix} \delta_{u_d} \\ \delta_{u_q} \\ \delta_{V} \\ \delta_{\beta_d} \end{bmatrix} \tag{3.3.8}$$

Fast Sub-system:

$$\begin{bmatrix} \dot{\delta_{i_d}} \\ \dot{\delta_{i_q}} \end{bmatrix} = \begin{bmatrix} -79.40 & 441.99 \\ -441.73 & -79.50 \end{bmatrix} \begin{bmatrix} \delta_{i_d} \\ \delta_{i_q} \end{bmatrix} + \begin{bmatrix} -24.06 & 0 & 0 & 0 \\ 0 & -24.06 & 0 & 0 \end{bmatrix} \begin{bmatrix} \delta_{u_d} \\ \delta_{u_q} \\ \delta_{V} \\ \delta_{\beta_d} \end{bmatrix} \tag{3.3.9}$$

3.4 Decoupling Results

The only way to verify the results of decoupling process using Chang's transformation is to compare the eigen values of the slow and fast sub-systes to those of the original composite system. **Eigen values of the slow sub-system are as follows:**

$$\left\{\begin{array}{l} p_{s1} = -3.58103127992448 + j35.5514815027664, \\ p_{s2} = -3.58103127992448 - j35.5514815027664, \\ p_{s3} = -0.685821687637942, \\ p_{s4} = -10 \end{array}\right\} \tag{3.4.1}$$

Eigen values of the fast sub-system are as follows:

$$\left\{\begin{array}{l} p_{f1} = -79.4506412894114 + j441.862874989898, \\ p_{f2} = -79.4506412894114 - j441.862874989898 \end{array}\right\} \tag{3.4.2}$$

Now by comparing the eigen values of original system in (3.3.5) with eigen values of slow and fast sub-systems in (3.4.1) and (3.4.2) we can say that they are almost equal with more than 99.8% accuracy, so we can say that the decoupling using chang's transform is reliable.

Original system	$p_1 = -3.58 + J35.55,$ $p_2 = -3.58 - j35.55,$ $p_3 = -0.68,$ $p_4 = -10$	$p_{s1} = -3.58 + J35.55,$ $p_{s2} = -3.58 - j35.55,$ $p_{s3} = -0.68,$ $p_{s4} = -10$	Slow Subsystem
	$p_5 = -79.45 + j441.86,$ $p_6 = -79.45 - j441.86$	$p_{f1} = -79.45 + j441.86,$ $p_{f2} = -79.45 - j441.86$	Fast Subsystem

Table 3.2: Eigen value comparision of Original system and Decomposed subsystems

3.5 Chapter Summary

In this chapter singular perturbation and time scales is presented and algorithm of Chang's transform is explained along with implementation on the selected system, to decompose a higher order system into two sub-systems based on the time scales and the process has been verified at the end by comparing the eigen values of the

original system and decomposed systems. The time scale nature of WECS was fully exploited by using dynamic decomposition approaches which provide a computationally inexpensive and flexible way to design controllers compared to the traditional way without decomposition of a higher order system.

4 Analysis and Design of VS-VP System

4.1 Introduction

In this chapter we will be discussing the design and analysis of Optimal LQR and Optimal LQG filters for the system [9]. The controllers are needed to be designed for each sub-system individually so, the controller is designed using the respective algorithms. The slow and fast subsystems obtained in the previous chapter are considered to design the filters in each case[35, 34, 37].

4.2 Optimal Linear Quadratic Regulator (LQR) Control

4.2.1 Optimal LQR Filter Design for the Original System

Considering the original linear system in (3.3.4) along with the cost function:

$$J = \int_0^\infty (X^T Q X + u^T R u) dt \tag{4.2.1}$$

where Q is a symmetric positive semi-definite matrix with dimensions $(m+n)$x$(m+n)$ m is number of slow satates in the system and n is number of fast states in the system,

and R is symmetric positive definite matrix with with dimensions rxr. Provided the system (A, B) is controllable, then according to optimal control theory the optimal control signal is given by:

$$u^* = -R^{-1}B^T\bar{P}X \tag{4.2.2}$$

where $R^{-1}B^T\bar{P}$ represent the optimal LQR filter (i.e. K) and $\bar{P}$ is the solution of the algebraic Riccati equation:

$$A^T\bar{P} + \bar{P}A - \bar{P}BR^{-1}\bar{P} + Q = 0 \tag{4.2.3}$$

To Implement above procedure to design an optimal LQR controller for the linear original (composite) system (3.3.4). Before implementing the procedure verifying, if the system fulfills the required condition of controllability. The controllability has been computed by MATLAB for the system which gives a full rank for the controllability matrix of the system (Rank=6) hence, the original system is controllable. The weighing matrices used for LQR function in MATLAB are:

$$Q = \begin{bmatrix} 1 & 0 & 0 & 0 & 0 & 0 \\ 0 & 1 & 0 & 0 & 0 & 0 \\ 0 & 0 & 1 & 0 & 0 & 0 \\ 0 & 0 & 0 & 1 & 0 & 0 \\ 0 & 0 & 0 & 0 & 1 & 0 \\ 0 & 0 & 0 & 0 & 0 & 1 \end{bmatrix}, R = \begin{bmatrix} 0.25 & 0 & 0 & 0 \\ 0 & 0.25 & 0 & 0 \\ 0 & 0 & 0.25 & 0 \\ 0 & 0 & 0 & 0.25 \end{bmatrix} \tag{4.2.4}$$

4.2.2 Optimal LQR Filter Design for the Slow Subsystem

Consider the System in (3.3.8) as:

$$\dot{X}_s = A_s X_s + B_s u_s \tag{4.2.5}$$

with the cost function:

$$J_s = \int_0^\infty (X_s^T Q_s X_s + u_s^T R_s u_s) dt \tag{4.2.6}$$

where Q_s is a symmetric positive semi-definite matrix with dimensions mxm, and R_s is symmetric positive definite matrix with with dimensions rxr. Provided the system (A_s, B_s) is controllable, then according to optimal control theory the optimal control signal is given by:

$$u_s^* = -R_s^{-1} B_s^T \bar{P}_s X_s \tag{4.2.7}$$

where $R_s^{-1} B_s^T \bar{P}_s$ represent the optimal slow LQR filter (i.e. K_s) and $\bar{P}_s$ is the solution of the algebraic Riccati equation:

$$A_s^T \bar{P}_s + \bar{P}_s A_s - \bar{P}_s B_s R_s^{-1} \bar{P}_s + Q_s = 0 \tag{4.2.8}$$

To implement above procedure to design an optimal LQR controller for the slow subsystem (3.3.8). Before implementing the procedure verifying, if the system fulfills the required condition of controllability. The controllability has been computed by MATLAB for the system which gives a full rank for the controllability matrix of the system (Rank=4) hence, the slow subsystem is controllable. The weighing matrices

used for slow LQR function in MATLAB are:

$$Q_s = \begin{bmatrix} 1 & 0 & 0 & 0 \\ 0 & 1 & 0 & 0 \\ 0 & 0 & 1 & 0 \\ 0 & 0 & 0 & 1 \end{bmatrix}, R_s = \begin{bmatrix} 0.25 & 0 & 0 & 0 \\ 0 & 0.25 & 0 & 0 \\ 0 & 0 & 0.25 & 0 \\ 0 & 0 & 0 & 0.25 \end{bmatrix} \tag{4.2.9}$$

4.2.3 Optimal LQR Filter Design for the Fast Subsystem

Consider the System in (3.3.9) as:

$$\dot{X}_f = A_f X_f + B_f u_f \tag{4.2.10}$$

with the cost function:

$$J_f = \int_0^\infty (X_f^T Q_f X_f + u_f^T R_f u_f) dt \tag{4.2.11}$$

where Q_f is a symmetric positive semi-definite matrix with dimensions nxn, and R_f is symmetric positive definite matrix with with dimensions rxr. Provided the system (A_f, B_f) is controllable, then according to optimal control theory the optimal control signal is given by:

$$u_f^* = -R_f^{-1} B_f^T \bar{P}_f X_f \tag{4.2.12}$$

where $R_f^{-1} B_f^T \bar{P}_f$ represent the optimal fast LQR filter (i.e. K_f) and $\bar{P}_f$ is the solution of the algebraic Riccati equation:

$$A_f^T \bar{P}_f + \bar{P}_f A_f - \bar{P}_f B_f R_f^{-1} \bar{P}_f + Q_f = 0 \tag{4.2.13}$$

To implement above procedure to design an optimal LQR controller for the fast subsystem (3.3.9). Before implementing the procedure verifying, if the system fulfills the required condition of controllability. The controllability has been computed by MATLAB for the system which gives a full rank for the controllability matrix of the system (Rank=2) hence, the fast subsystem is controllable. The weighing matrices used for fast LQR function in MATLAB are:

$$Q_f = \begin{bmatrix} 1 & 0 \\ 0 & 1 \end{bmatrix}, R_f = \begin{bmatrix} 0.25 & 0 & 0 & 0 \\ 0 & 0.25 & 0 & 0 \\ 0 & 0 & 0.25 & 0 \\ 0 & 0 & 0 & 0.25 \end{bmatrix} \tag{4.2.14}$$

Now, after obtaining slow and fast optimal LQR control signals, composite optimal control signal can be obtained as shown in the figure below by:

$$u_c^* = u_f^* + u_s^* \tag{4.2.15}$$

The implementation diagram of the reduced-order LQR optimal control and original LQR optimal control is shown in Fig. 4.1 where two independent, reduced-order optimal controllers are obtained using the time scale decomposition and optimal control theory. The overall composite control is a composite of two reduced-order LQR optimal controls, u_s and u_f , as indicated in (4.2.15). And as we have seen before that eigen values of original system and the decomposed sub-systems are same so it is safe to say that:

$$u^* \approx u_c^* \tag{4.2.16}$$

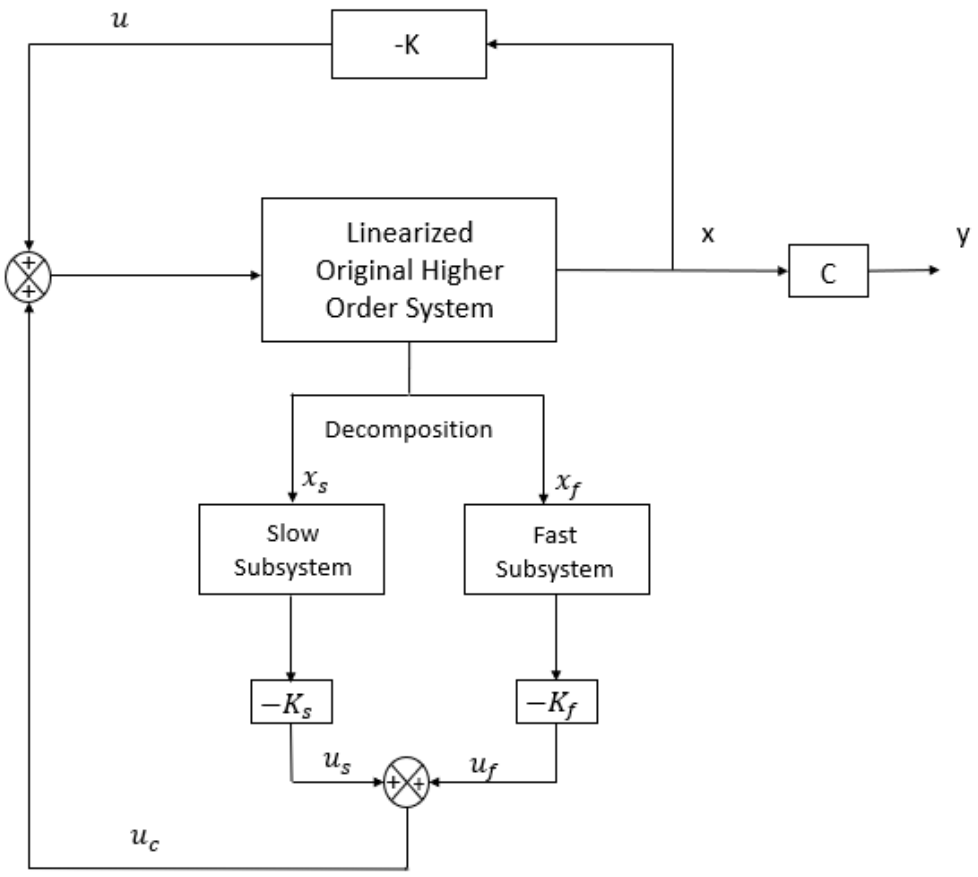

Figure 4.1: Time Scale LQR control diagram

4.3 Optimal Linear Quadratic Guassian (LQG) Control

In this section Optimal controller is designed for the PMSG-based WECS using optimal LQG control theory, which is much suited for stochastic situations, so it will be best suited for WECS problems as all the WECS are operated in undeterministic wind conditions which change stochastically all the time along with the environment. In this section the methods for designing controllers for both original system and singularly perturbed linear PMSG-based WECS are presented.

4.3.1 Decoupling Kalman Filter Design

The study for designing filters for singularly perturbed systems has been studied [16] and in the study several methods have been proposed to decompose a Kalman filter for a singularly perturbed system, and decomposing Kalman filter with high accuracy has only been achieved by two methods. First method is called classic method but, it does not provide slow and fast decomposed Kalman filters independent of one another computationally. Second method solves this problem by providing slow and fast filters of the singularly perturbed system independent of one another. In this section second method is discussed briefly. For more detail regarding the methods refer to [16]

A linear singularly perturbed in a stochastic environment with stochastic noise can be represented by:

$$\dot{X}_1 = A_1 X_1 + A_2 X_2 + G_1 w_1, \tag{4.3.1}$$

$$\epsilon \dot{X}_2 = A_3 X_1 + A_4 X_2 + G_2 w_1, \tag{4.3.2}$$

$$y = C_1 X_1 + C_2 X_2 + w_2 \tag{4.3.3}$$

where X_1, X_2 are m and n dimensional state vectors, respectively and w_1 w_2 are process and measurement white Guassian noises with intensities W_1 and W_2, respectively. $A_{1-4}, G_{1-2}, B_{1-2} and C_{1-2}$ are constant matrices. The slow and fast Kalman filters are given by:

$$\dot{\hat{X}}_s = \hat{A}_s \hat{X}_s + K_s y, \tag{4.3.4}$$

$$\dot{\hat{X}}_f = \hat{A}_f \hat{X}_f + K_f y \tag{4.3.5}$$

where

$$\hat{A}_s = (a_{1F} + a_{2F} P_{sF})^T, \tag{4.3.6}$$

$$\hat{A}_f = (b_{1F} + b_{2F} P_{fF})^T \tag{4.3.7}$$

K_s and K_f are the slow and fast Kalman filter coefficients, respectively. The computaions of $\hat{A}_s$ and $\hat{A}_f$ involve solutions of Chang"s decoupling equation:

$$T_{4F} M - T_{3F} - \epsilon M (T_{1F} - T_{2F} M) = 0, \tag{4.3.8}$$

$$T_{2F} - N(T_{4F} + \epsilon M T_{2F}) + \epsilon (T_{1F} - T_{2F} M) N = 0 \tag{4.3.9}$$

where

$$T_{1F} = \begin{bmatrix} A_1^T & -C_1^T W_2^{-1} C_1 \\ -G_1 W_1 G_1^T & -A_1 \end{bmatrix} \tag{4.3.10}$$

$$T_{2F} = \begin{bmatrix} A_3^T & -C_1^T W_2^{-1} C_2 \\ -G_1 W_1 G_2^T & -A_2 \end{bmatrix} \tag{4.3.11}$$

$$T_{3F} = \begin{bmatrix} A_2^T & -C_2^T W_2^{-1} C_1 \\ -G_2 W_1 G_1^T & -A_3 \end{bmatrix} \tag{4.3.12}$$

$$T_{4F} = \begin{bmatrix} A_4^T & -C_2^T W_2^{-1} C_2 \\ -G_2 W_1 G_2^T & -A_4 \end{bmatrix} \tag{4.3.13}$$

These equations can be solved to get the solutions for M and N using recursive algorithms (Fixed Point Algorithm or Newtons Algorithm) explained in (3.2.2). The matrices $a_{1F}, a_{2F}, b_{1F}, b_{2F}$ in equations (4.3.6) and (4.3.7) can be calculated by:

$$\begin{bmatrix} a_{1F} & a_{2F} \\ a_{3F} & a_{4F} \end{bmatrix} = (T_{1F} - T_{2F} M) \tag{4.3.14}$$

$$\begin{bmatrix} b_{1F} & b_{2F} \\ b_{3F} & b_{4F} \end{bmatrix} = (T_{4F} + \epsilon M T_{2F}) \tag{4.3.15}$$

And the matrices P_{sF} and P_{fF} in equations (4.3.6) and (4.3.7) are the slow and fast filters (i.e. solution) for algebraic Riccati equations:

$$P_{sF} a_{1F} - a_{4F} P_{sF} - a_{3F} + P_{sF} a_{2F} P_{sF} = 0, \tag{4.3.16}$$

$$P_{fF} b_{1F} - b_{4F} P_{fF} - b_{3F} + P_{fF} b_{2F} P_{fF} = 0 \tag{4.3.17}$$

P_{sF} and P_{fF} are given by the solution of Sylvester Equations:

$$\begin{aligned} &P_{sF}(k+1)(a_{1F} + a_{2F} P_{sF}(k)) \\ -&(a_{4F} - P_{sF}(k) a_{2F}(k)) P_{sF}(k+1) = a_{3F} + P_{sF}(k) a_{2F} P_{sF}(k), \\ &k = 0, 1, 2, ... \end{aligned} \tag{4.3.18}$$

$$
\begin{aligned}
&P_{fF}(k+1)(b_{1F}+b_{2F}P_{fF}(k)) \\
-(b_{4F}-P_{fF}(k)b_{2F}(k))&P_{fF}(k+1)=b_{3F}+P_{fF}(k)b_{2F}P_{fF}(k), \\
&k=0,1,2,...
\end{aligned} \tag{4.3.19}
$$

The initial guess for (4.3.18) is the solution of algebraic Riccati equation:

$$
P_{sF}(0)A_{sF}^T+A_{sF}P_{sF}(0)+G_sW_{1s}G_s^T-P_{sF}(0)C_s^TW_{2s}^{-1}C_sP_{sF}(0)=0 \tag{4.3.20}
$$

where $A_{sF}, C_s, G_s, W_{1s}, W_{2s}$ can be computed by:

$$
\begin{bmatrix} A_{sF}^T & -C_s^TW_{2s}^{-1}C_s \\ -G_sW_{1s}^{-1}G_s^T & A_{sF} \end{bmatrix} = T_{1F}-T_{2F}T_{4F}^{-1}T_{3F} \tag{4.3.21}
$$

And the initial guess for (4.3.19) is the solution of algebraic Riccati equation:

$$
P_f(0)A_4^T+A_4P_f(0)+G_2W_1G_1^T-P_f(0)C_1^TW_2^{-1}C_2P_f(0)=0 \tag{4.3.22}
$$

The Kalman filter coefficients K_s and K_f are given by:

$$
\begin{bmatrix} K_s \\ \frac{1}{\epsilon}K_f \end{bmatrix} = T_2^{-T}\begin{bmatrix} K_1 \\ \frac{1}{\epsilon}K_2 \end{bmatrix} \tag{4.3.23}
$$

where T_2 is a linear transformation given by:

$$
\begin{bmatrix} \hat{X}_s & \hat{X}_f \end{bmatrix} = T_2^{-T}\begin{bmatrix} \hat{X}_1 \\ \hat{X}_2 \end{bmatrix} \tag{4.3.24}
$$

And K_1 and K_2 are optimal Kalman filters given by:

$$K_1 = (P_{1F}C_1^T + P_{2F}C_2^T)W_2^{-1}, \tag{4.3.25}$$

$$K_2 = (\epsilon P_{2F}^T C_1^T + P_{3F}C_2^T)W_2^{-1} \tag{4.3.26}$$

where $P_{1F}, P_{2F} and P_{3F}$ are obtained from the solution of algebraic Riccati equation:

$$AP_F + P_F A^T - P_F S P_F + G W_1 G^T = 0 \tag{4.3.27}$$

where

$$A = \begin{bmatrix} A_1 & A_2 \\ \frac{1}{\epsilon}A_3 & \frac{1}{\epsilon}A_4 \end{bmatrix}, \tag{4.3.28}$$

$$G = \begin{bmatrix} G_1 \\ \frac{1}{\epsilon}A_2 \end{bmatrix}, \tag{4.3.29}$$

$$S = C^T W_2^{-1} C, \tag{4.3.30}$$

$$P_F = \begin{bmatrix} P_{1F} & P_{2F} \\ P_{2F}^T & \frac{1}{\epsilon}P_{3F} \end{bmatrix} \tag{4.3.31}$$

The linear transformation T_2 is given as:

$$T_2 = (\Pi_{1F} + \Pi_{2F} P_F) \tag{4.3.32}$$

where

$$\Pi_F = \begin{bmatrix} \Pi_{1F} & \Pi_{2F} \\ \Pi_{3F} & \Pi_{4F} \end{bmatrix} = E_{2F}^T \begin{bmatrix} I_2 - \epsilon NM & -\epsilon N \\ M & I_{2n} \end{bmatrix} E_{1F} \tag{4.3.33}$$

M and N are solution of the equations (4.3.8) and (4.3.9), and:

$$E_{1F} = \begin{bmatrix} I_m & 0 & 0 & 0 \\ 0 & 0 & I_m & 0 \\ 0 & \frac{1}{\epsilon} I_n & 0 & 0 \\ 0 & 0 & 0 & I_n \end{bmatrix}, \tag{4.3.34}$$

$$E_{2F} = \begin{bmatrix} I_m & 0 & 0 & 0 \\ 0 & 0 & I_m & 0 \\ 0 & I_n & 0 & 0 \\ 0 & 0 & 0 & I_n \end{bmatrix}, \tag{4.3.35}$$

4.3.2 Optimal LQG Control Design

In this section LQG filter design for singularly perturbed system in a stochastic environment (i.e like the one in unpredictable wind) in [16] is explained in detail. The filter design is based on decomposing the Kalman filter.

Consider a singularly perturbed linear continuous system:

$$\dot{X}_1 = A_1 X_1 + A_2 X_2 + G_1 w_1, \tag{4.3.36}$$

$$\epsilon \dot{X}_2 = A_3 X_1 + A_4 X_2 + G_2 w_1, \tag{4.3.37}$$

$$y = C_1 X_1 + C_2 X_2 + w_2 \tag{4.3.38}$$

where X_1, X_2 are m and n dimensional state vectors, respectively and w_1 w_2 are process and measurement white Guassian noises with intensities W_1 and W_2, respectively. $A_{1-4}, G_{1-2}, B_{1-2} and C_{1-2}$ are constant matrices. The cost function is given by:

$$J = \lim_{t_f \to \infty} \frac{1}{t_f} E \left\{ \int_{t_0}^{t_f} [Z^T Z + u^T R u] dt \right\} \tag{4.3.39}$$

where t_0 and t_f are initial time and final time respectively,$z = Q_{1F} X_1 + Q_{2F} X_2$ is a controlled output, where $Q_{1F} \geq 0$ and $Q_{2F} \geq 0$ are state weighing matrices, and $R > 0$ is control weighing matrix. Optimal control law for the system (4.3.36), (4.3.37) and (4.3.38) is given in terms of slow and fast Kalman Filters as:

$$u^* = -F\hat{X} = -F_s \hat{X}_s - -F_f \hat{X}_f = u_s^* + u_f^* \tag{4.3.40}$$

where F_s and F_f are slow and fast regulator gains, respectively, and X_s and X_f are slow and fast states. Slow and fast Kalman filters are give by:

$$\dot{\hat{X}}_s = \hat{A}_s \hat{X}_s + B_s u + K_s y, \tag{4.3.41}$$

$$\epsilon \dot{\hat{X}}_f = \hat{A}_s \hat{X}_f + B_f u + K_f y, \tag{4.3.42}$$

where $\hat{A}_s$ and $\hat{A}_f$ are given by (4.3.6) and (4.3.7) respectively, K_s and K_f are given

by (4.3.23) and B_s and B_f is calculated by:

$$\begin{bmatrix} B_s \\ \frac{1}{\epsilon}B_f \end{bmatrix} = T_2^T \begin{bmatrix} B_1 \\ \frac{1}{\epsilon}B_2 \end{bmatrix} \tag{4.3.43}$$

with T_2 given by:

$$[F_s F_f] = FT_2^T = R^{-1}B^T P(\Pi_{1F} + \Pi_{2F}P_F)^T \tag{4.3.44}$$

where P_F is the solution of the Algebraic Riccati Equation (4.3.27) and P is the solution of Algebaric ricatti equation given by:

$$PA + A^T P + Q - PBR^{-1}B^T P = 0. \tag{4.3.45}$$

The optimal value of cost function is

$$J^* = tr\left\{PGW_1G^T + P_F F^T RF\right\} \tag{4.3.46}$$

The implementation diagrams of the reduced order LQG filtering and control is shown below in Figure 4.2 where two independent reduced order filters are used to estimate the slow and fast state vectors based on the system output, y, and control input, u. The overall control is a composite of two reduced-order LQG optimal controls, u_s and u_f , as indicated in (4.3.40).

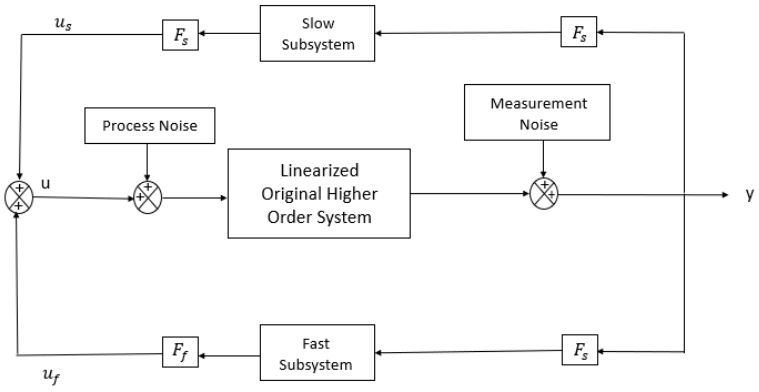

Figure 4.2: LQG Control Diagram

4.4 Summary

In this chapter two of the most prominent optimal control techniques LQR and LQG are explained in detail with step by step description to obtain corresponding optimal control filters for original system and then for singularly perturbed slow and fast subsystems. In the next chapter, the simulation results of each technique are presented which have been implemented in MATLAB to compare the results of each technique original optimal control filter results with the results of two seperate filters for both slow and fast subsystem.

5 Results

5.1 Introduction

In this chapter the simulation results of the different optimal control techniques that have been explained in the previous chapter for both original system and the singularly perturbed slow and fast sub-systems, both the results are compared in case of each control technique. An analysis is also done to check if, implementation of time scales and designing of the individual optimal control filters for the subsystem has improved the performance by comparing and analyzing the simulation results.

5.2 Optimal LQR Control Simulation Results

The Optimal LQR theory explained in the previous chapter and the filter obtained for the system in the section 4.2 has been applied to to the original system and singularly perturbed slow and fast subsystems of the Grid connected PMSG-based system from state-space equations (3.3.4), (3.3.8) and (3.3.9) are simulated in MATLAB and SIMULINK environment to compare the results. The simlation results are as shown below in each case

5.2.1 Optimal LQR Control and Simulation Results for Original System

LQR filter is designed for the original system in equation (3.3.4) using the control theory explained in section 4.2.1 and the optimal gain computed by MATLAB using *lqr* function using the weighing matrices from equation (4.2.4) is as follows:

$$K = \begin{bmatrix} 1.2535 & -0.5609 & 0.0087 & -0.0267 & -0.5657 & 0.0015 \\ -0.2687 & 0.1038 & -0.0133 & 0.0019 & 0.0015 & -0.5587 \\ 0 & 0 & 0 & 0 & 0 & 0 \\ -15.8572 & 0.9702 & 0.5783 & 2.2907 & 0.0111 & -0.0008 \end{bmatrix} \tag{5.2.1}$$

Simulation Results Graph for Original System using LQR filter

All the states of the system (3.3.4) are fed back through the filter (K) designed in the equation above (5.2.1) with the initial conditions of all the states as zeroes and the resulting responses are shown in the Figure 5.1. below:

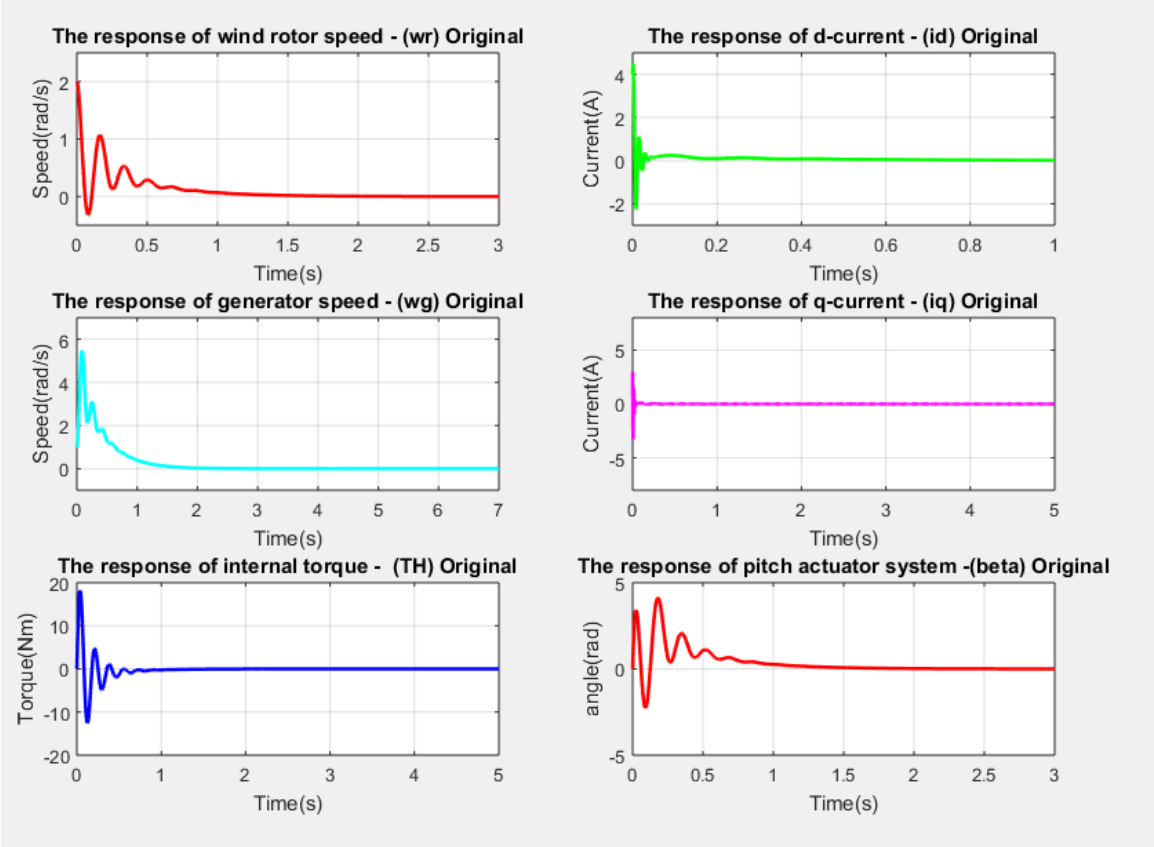

Figure 5.1: LQR Original System Results

5.2.2 Optimal LQR Control and Simulation Results for Slow and Fast Subsystems

LQR filter is designed for the Singularly perturbed slow subsystem in equation (3.3.8) using the control theory explained in section 4.2.2 and the optimal gain computed by MATLAB using *lqr* function for the slow subsystem using the weighing

matrices from equation (4.2.9) is as follows:

$$K_s = \begin{bmatrix} -0.6810 & -1.5031 & 1.8406 & 0.3522 \\ 0.1224 & 0.2702 & -0.33085 & -0.0633 \\ 0 & 0 & 0 & 0 \\ -5.1697 & 0.0172 & 0.0574 & 1.6202 \end{bmatrix} \tag{5.2.2}$$

similarly LQR filter is designed for fast subsystem in equation (3.3.9) using the equations and control theory in section 4.2.3 and the optimal gain computed by MATLAB using *lqr* function for using the weighing matrices from equation (4.2.14) is calculated as:

$$K_f = \begin{bmatrix} -0.5583 & -0.00009 \\ -0.00009 & -0.5583 \\ 0 & 0 \\ 0 & 0 \end{bmatrix} \tag{5.2.3}$$

Simulation Results Graph for Slow and Fast Subsystem using corresponding LQR filters for each subsystem

All the states of the system (3.3.8) and (3.3.9) are fed back through the slow subsystem filter (K_s) and fast subsystem filter (K_f) respectively designed in the equations (5.2.2) and (5.2.3) with the initial conditions of all the states as zeroes and the resulting responses are shown in the Figure 5.2. below: In the graphs the responses of all the slow states ω_r, ω_g, T_H and *beta* are corresponding to the slow subsystem filter (i.e. K_s) and responses of fast subsystem states i_d and i_q are corresponding to fast filter (i.e. K_f).

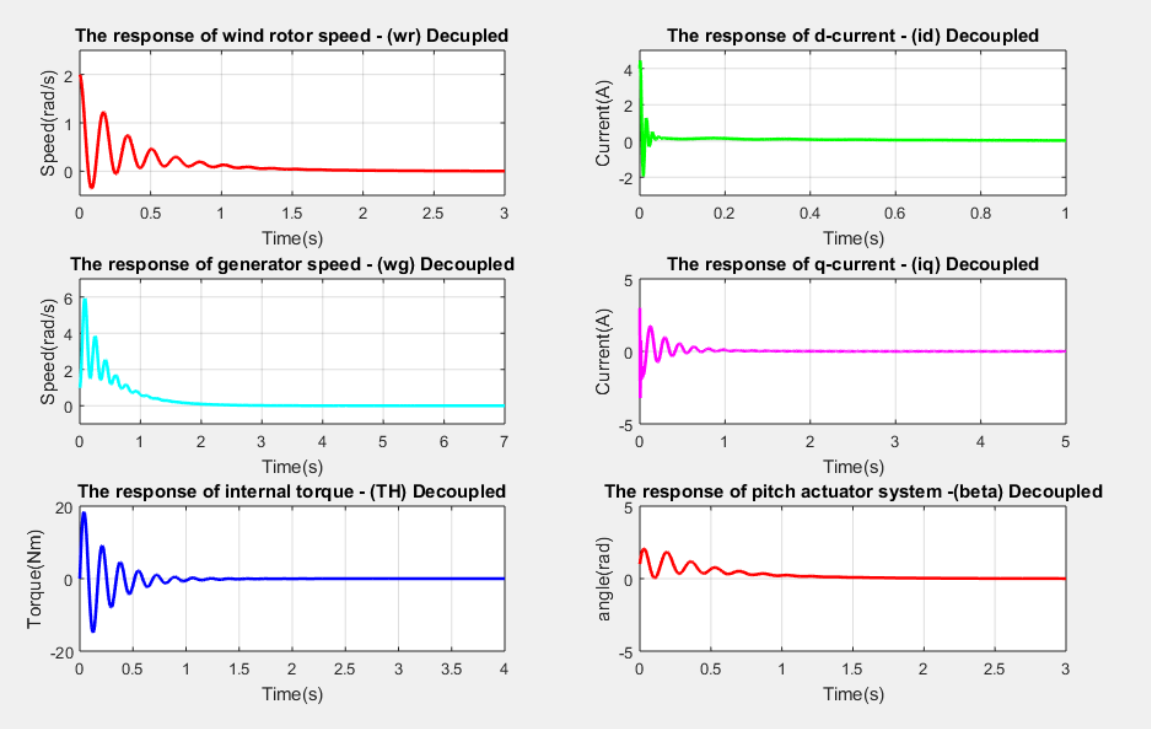

Figure 5.2: LQR Decoupled System Results

5.2.3 Comparision of Responses of Each State

In the following graphs all responses of the states in original system are compared to corresponding responses of the states in singularly perturbed slow and fast subsystems

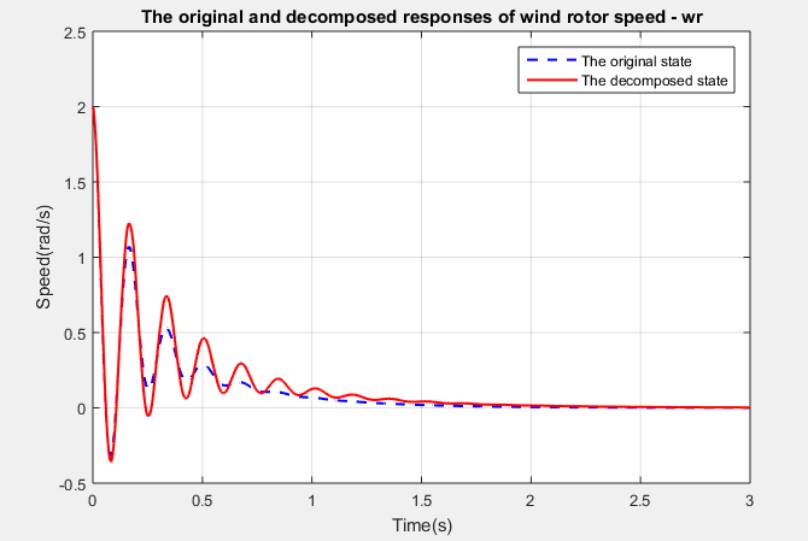

Figure 5.3: Comparision of Angular Velocity of Rotor (ω_r)

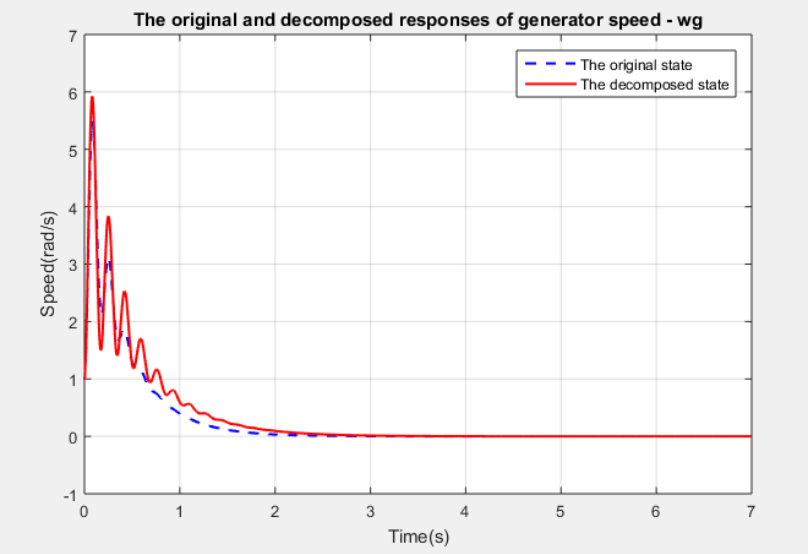

Figure 5.4: Comparision of Angular Velocity of Generator (ω_g)

5.3 Optimal LQG Control Simulation Results

In this section the optimal LQG theory explained in section 4.3 is implemented on the the original and singularly perturbed systems in (3.3.4), (3.3.8) and (3.3.9) using MATLAB and SIMULINK and the results calculated With the initial conditions for

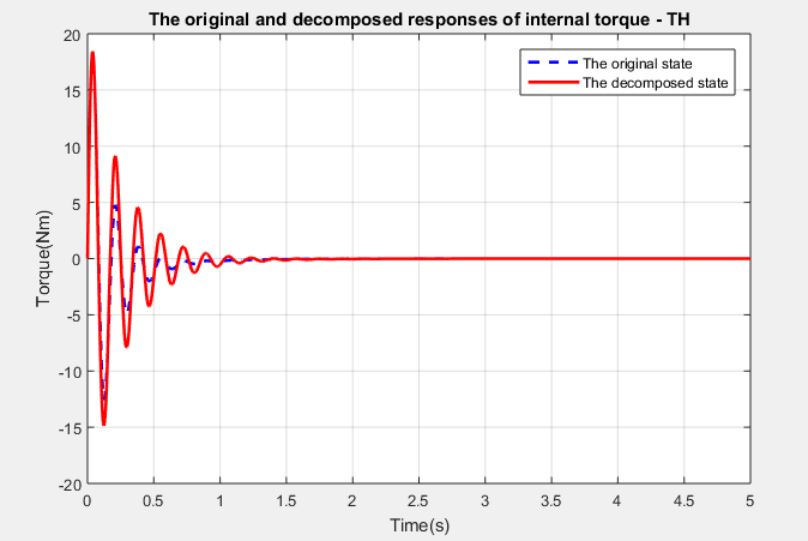

Figure 5.5: Comparision of Internal Torque (T_H)

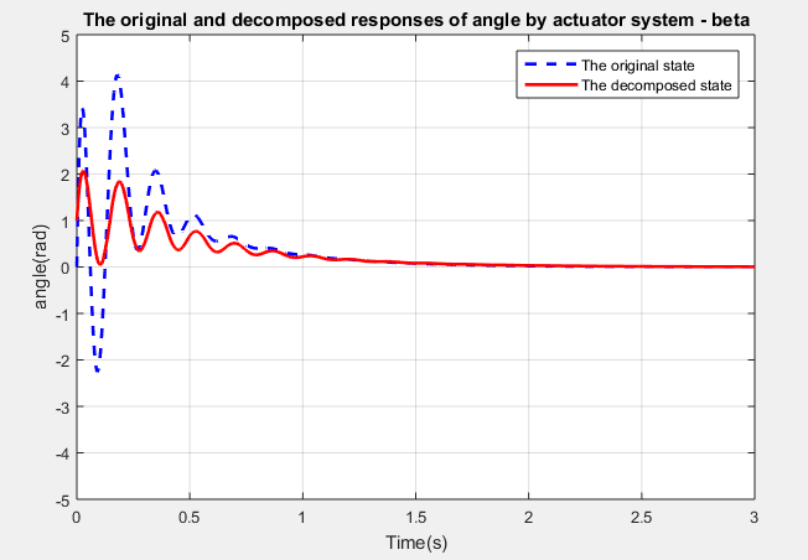

Figure 5.6: Comparision of Pitch Angle (β)

all the states as zero and simulations are explained and compared to one another.

5.3.1 Optimal LQG Control Simulation Results

All the results obtained for all the matrices and arithematic ricatti equation for the system in equation (3.3.4) are as follows:

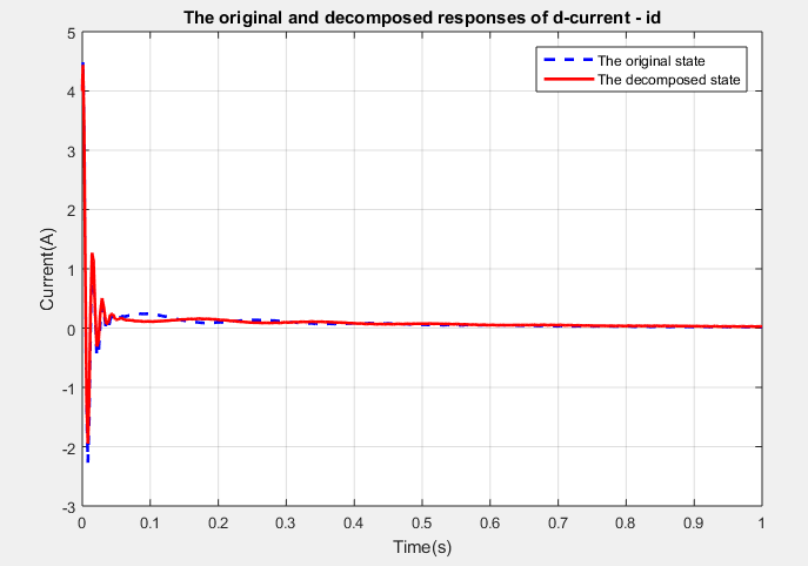

Figure 5.7: Comparision of d-component of stator current in PMSG (i_d)

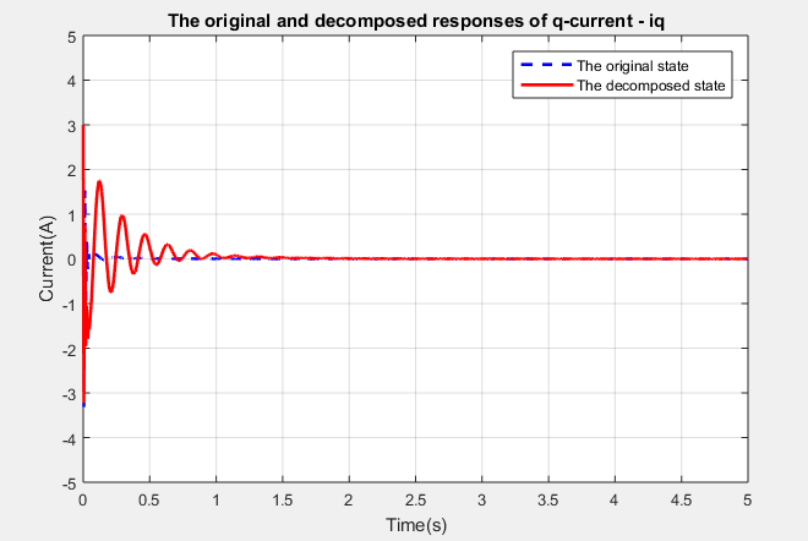

Figure 5.8: Comparision of q-component of stator current in PMSG (i_q)

Considering only single state for the output

$$C = [C_1 C_2] = \begin{bmatrix} 1 & 0 & 0 & 0 & 0 & 0 \end{bmatrix} \tag{5.3.1}$$

where

$$C_1 = \begin{bmatrix} 1 & 0 & 0 & 0 \end{bmatrix}, C_2 = \begin{bmatrix} 0 & 0 \end{bmatrix} \tag{5.3.2}$$

Also considering the process and measurement noises as $W_1 = W_2 = 1$. The solution for Chang's decoupling equations (4.3.8) and (4.3.9) is:

$$M = \begin{bmatrix} 0.0088 & -7.6055 & 1.8566 & 0 & 0 & 0 & 0 & 0 \\ 0.0072 & 1.3496 & -1.6122 & 0 & 0 & 0 & 0 & 0 \\ 0 & 0 & -0.0002 & 0 & 0.0004 & -0.0443 & 0 & 0 \\ 0 & 0.0008 & -0.002 & 0 & 0 & 0.0158 & -0.0004 & 0 \end{bmatrix} \tag{5.3.3}$$

and

$$N = \begin{bmatrix} 0.0004 & 0 & 0 & 0 \\ -0.0443 & 0.0158 & 0 & 0 \\ 0 & -0.0004 & 0 & 0 \\ 0 & 0 & 0 & 0 \\ 0 & 0 & 0.0088 & 0.0072 \\ 0 & -0.0008 & -7.6008 & 1.3488 \\ 0.0002 & 0.0002 & 1.8552 & -1.6119 \\ 0 & 0 & 0 & 0 \end{bmatrix} \tag{5.3.4}$$

Matrices a_{1F} and a_{2F} from equation (4.3.14) are calculated as:

$$a_{1F} = \begin{bmatrix} -2.7453 & 0 & 445.0584 & 0 \\ -0.0004 & 0.0955 & -74.9828 & 0 \\ -2.0833 & 4.5455 & -5.1136 & 0 \\ -3.3771 & 0 & -6.0788 & -10 \end{bmatrix} \tag{5.3.5}$$

$$a_{2F} = \begin{bmatrix} -3.3333 & 0 & 0 & 0 \\ 0 & 0 & 0 & 0 \\ 0 & 0 & 0 & 0 \\ 0 & 0 & 0 & 0 \end{bmatrix} \tag{5.3.6}$$

Matrices b_{1F} and b_{2F} from equation (4.3.14) are calculated as:

$$b_{1F} = \begin{bmatrix} -0.1374 & -0.7634 \\ 0.7630 & 0.1371 \end{bmatrix} \tag{5.3.7}$$

$$b_{2F} = 10^{-8}X \begin{bmatrix} 0 & -0.1075 \\ 0 & -0.1045 \end{bmatrix} \tag{5.3.8}$$

Solution for P_{sf} and P_{fF} for the slow and fast ricatti equation s in (4.3.16) and (4.3.17) are computed as:

$$P_{sF} = \begin{bmatrix} 0.5192 & 0.9596 & 0.9011 & -0.0229 \\ 0.9590 & 10.4436 & 0.1174 & -0.1055 \\ 0.9012 & 0.1194 & 79.0570 & -0.2461 \\ -0.0229 & -0.1056 & -0.2461 & 0.2499 \end{bmatrix}, P_{fF} = 10^{-3} \begin{bmatrix} 0.3146 & 0 \\ -0.0001 & 0.3146 \end{bmatrix} \tag{5.3.9}$$

The slow and fast Kalman filter coefficients in equation (4.3.23) are obtained as:

$$K_s = \begin{bmatrix} 1.7308 \\ 3.1985 \\ 3.0035 \\ -0.0763 \end{bmatrix}, K_f = 1^{-10} \begin{bmatrix} -1.223 \\ -0.3760 \end{bmatrix} \tag{5.3.10}$$

The slow ($\hat{A}_s$) and fast system ($\hat{A}_f$) matrices obtained from equations (4.3.6) and (4.3.7) of Kalman filtering are :

$$\hat{A}_s = \begin{bmatrix} -4.4761 & -0.0004 & -2.0833 & -3.3771 \\ -3.1985 & 0.0955 & 4.5455 & 0 \\ 442.0549 & -74.9828 & -5.1136 & -6.0788 \\ 0.0763 & 0 & 0 & -10 \end{bmatrix} \tag{5.3.11}$$

$$\hat{A}_f = \begin{bmatrix} -0.1374 & 0.7630 \\ -0.7634 & -0.1371 \end{bmatrix} \tag{5.3.12}$$

Slow and fast input matrices B_s and B_f calculated are as follows:

$$B_s = \begin{bmatrix} 0.0004 & 0.0003 & 0 & 0 \\ -0.3161 & 0.0561 & 0 & 0 \\ 0.0772 & -0.0670 & 0 & 0 \\ 0 & 0 & 0 & 10 \end{bmatrix} \tag{5.3.13}$$

$$B_f = 10^{-4} \begin{bmatrix} -0.7174 & -0.0001 & 0 & 0 \\ -0.0002 & -0.7178 & 0 & 0 \end{bmatrix} \tag{5.3.14}$$

And the slow and fast regulator gains F_s and F_f from equation (4.3.44) are computed as:

$$F_s = \begin{bmatrix} 4.7630 & -3.2576 & 0.0829 & -0.1909 \\ -2.0986 & 1.1896 & -0.0945 & 0.0776 \\ 0 & 0 & 0 & 0 \\ -67.4661 & 6.4325 & -1.1252 & 8.3751 \end{bmatrix} \tag{5.3.15}$$

$$F_f = 10^{-3} \begin{bmatrix} -2.1951 & -0.0040 \\ -0.0090 & -2.2173 \\ 0 & 0 \\ -0.0516 & 0.0100 \end{bmatrix} \tag{5.3.16}$$

Kalman filter has been decomposed into slow and fast Kalman filters and then fed into slow and fast optimal regulator gains for simulation as shown in the Figure 4.2 and the simulation results for one of the states is as follows:

Figure 5.9 has all the state estimates for the original system when passed through the LQG filter.

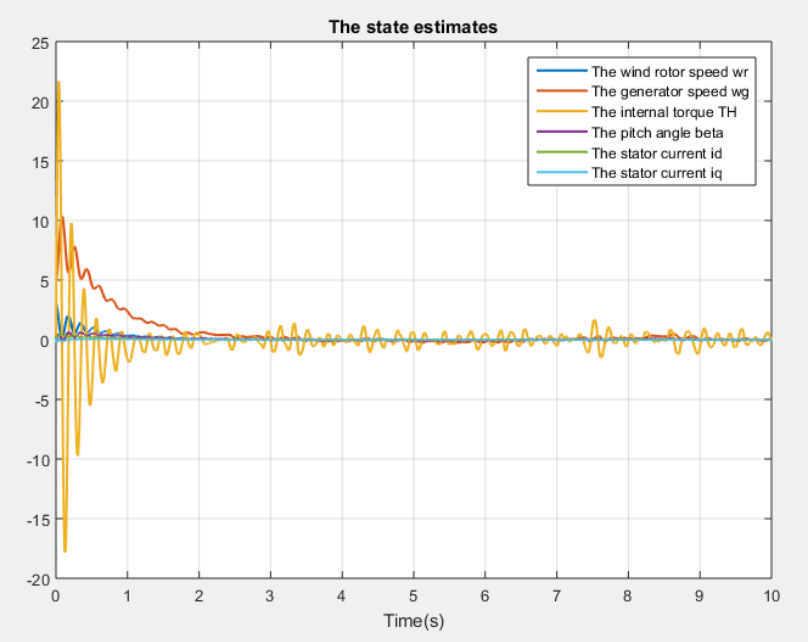

Figure 5.9: State Estimates for LQG Original System (i_q)

Figure 5.10 below has the state estimate for Angular velocity for the rotor ω_r scaled to proper size for the original system. Figure 5.11 shows the state estimate for

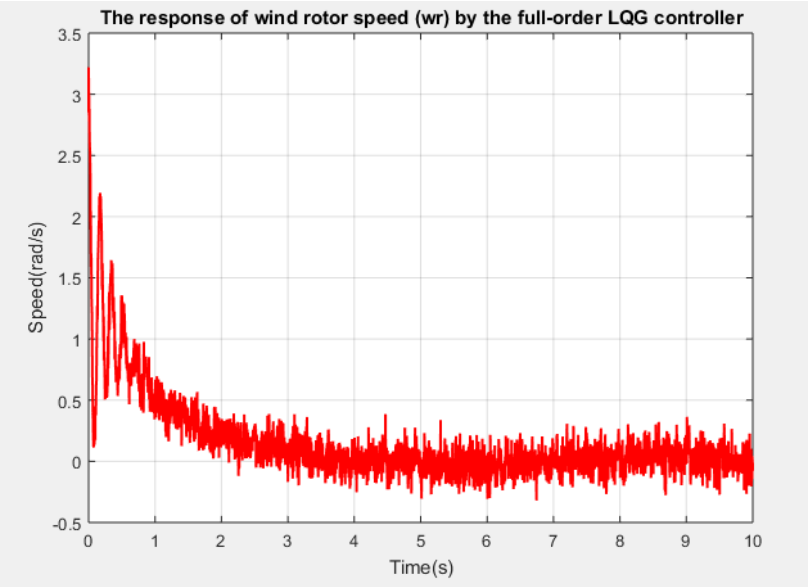

Figure 5.10: Response for (ω_r) original system

Angular velocity for the rotor ω_r scaled to proper size for the decomposed system.

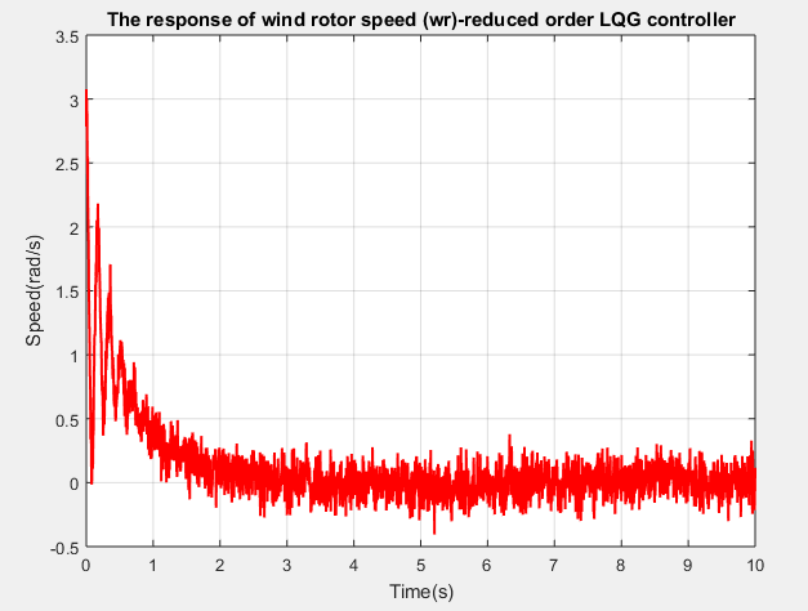

Figure 5.11: Response for (ω_r) decomposed system

Figure 5.12 has both of the above graphs for comparison of response for ω_r of original system to that of reduced order system (i.e. Decomposed system). And

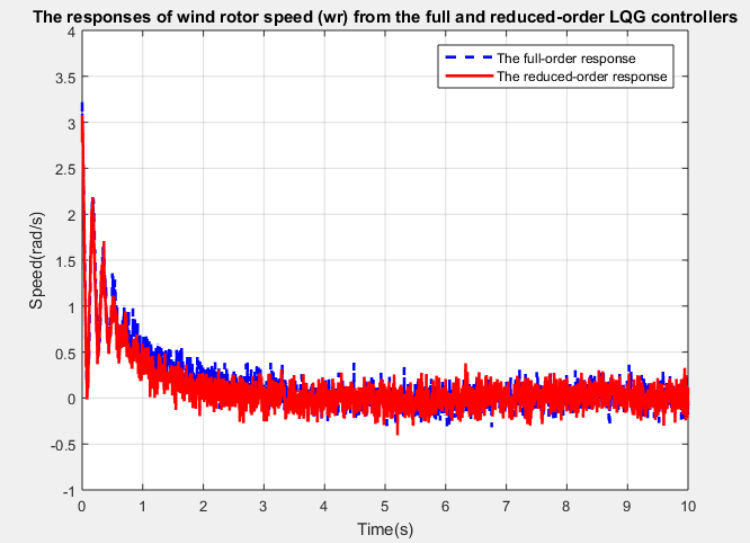

Figure 5.12: Difference between the Responses for (ω_r)

Figure 5.13 has the difference between control signals generated by LQG control loops of original system and decomposed system for ω_r. Figure 5.14 shows the state

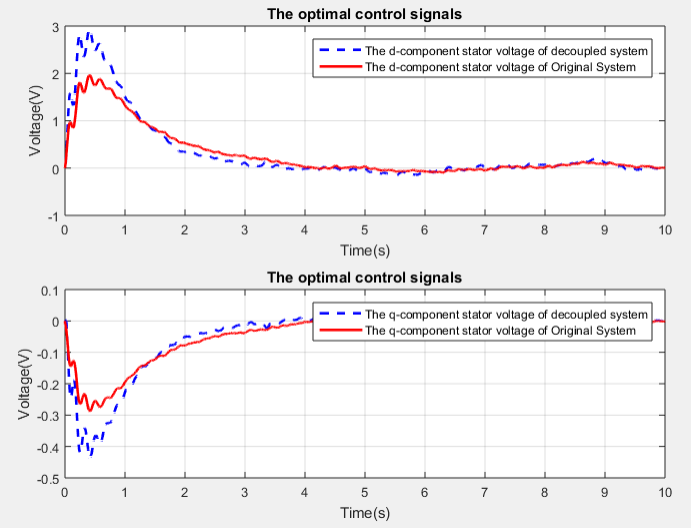

Figure 5.13: Difference between the Control signals for ω_r

estimate for Angular velocity for the PMSG ω_g scaled to proper size for the original

system. Figure 5.15 shows the state estimate for Angular velocity for the PMSG ω_g

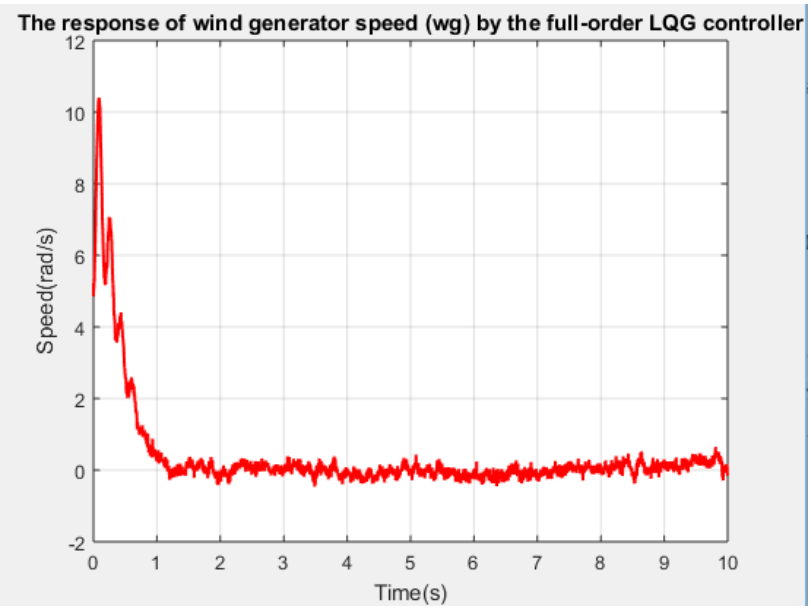

Figure 5.14: Response for (ω_g) original system

scaled to proper size for the decomposed system. Figure 5.16 has both of the above graphs for comparison of response for ω_g of original system to that of reduced order system (i.e. Decomposed system). And Figure 5.17 has the difference between control signals generated by LQG control loops of original system and decomposed system for ω_g.

Figure 5.18 shows the state estimate for Internal Torque (T_H) scaled to proper size for the original system. Figure 5.19 shows the state estimate for Internal Torque (T_H) scaled to proper size for the decomposed system. Figure 5.20 has both of the above graphs for comparison of response for Internal Torque (T_H) of original system to that of reduced order system (i.e. Decomposed system). And Figure 5.21 has the difference between control signals generated by LQG control loops of original system and decomposed system for Internal Torque (T_H).

Figure 5.22 shows the state estimate for Pitch Angle (β) scaled to proper size for

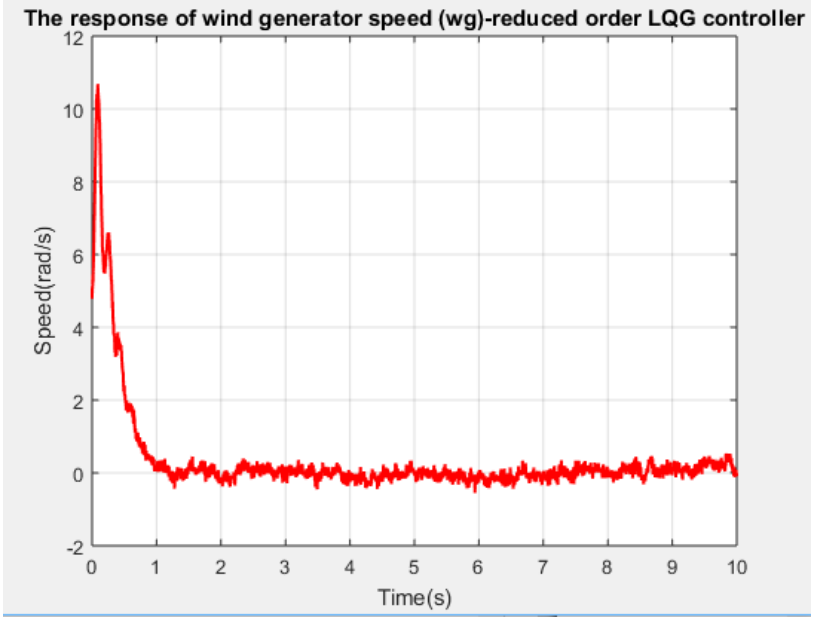

Figure 5.15: Response for (ω_g) decomposed system

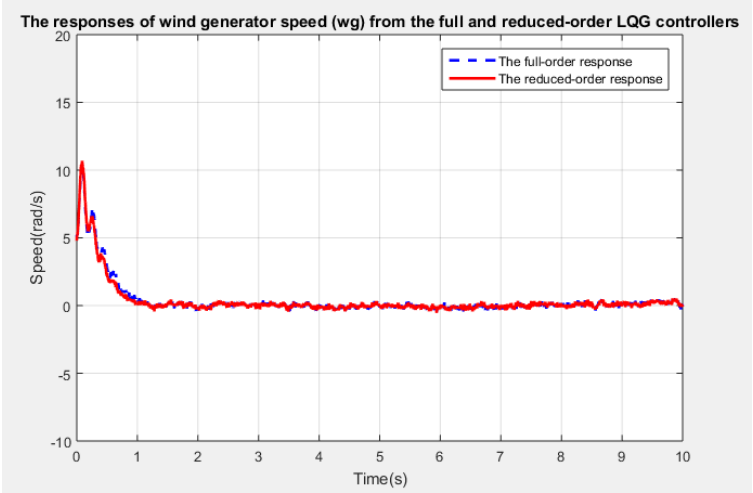

Figure 5.16: Difference between the Responses for (ω_g)

the original system. Figure 5.23 shows the state estimate for Pitch Angle (β) scaled to proper size for the decomposed system. Figure 5.24 has both of the above graphs for comparison of response for Pitch Angle (β) of original system to that of reduced order system (i.e. Decomposed system). And Figure 5.25 has the difference between control signals generated by LQG control loops of original system and decomposed

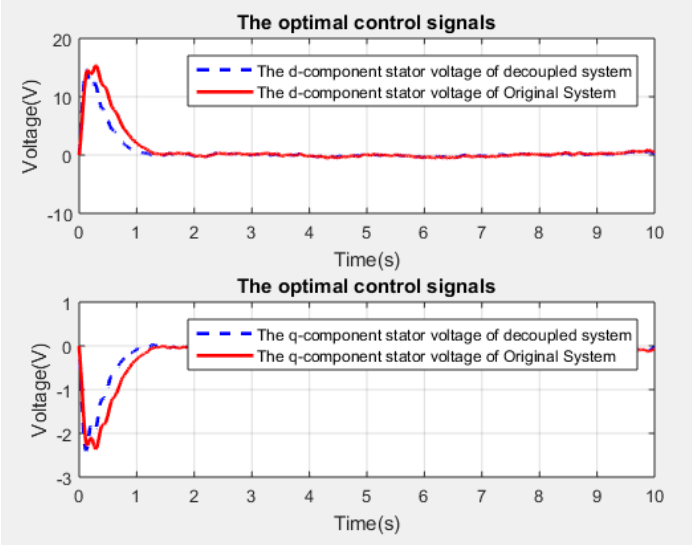

Figure 5.17: Difference between the Control signals for ω_g

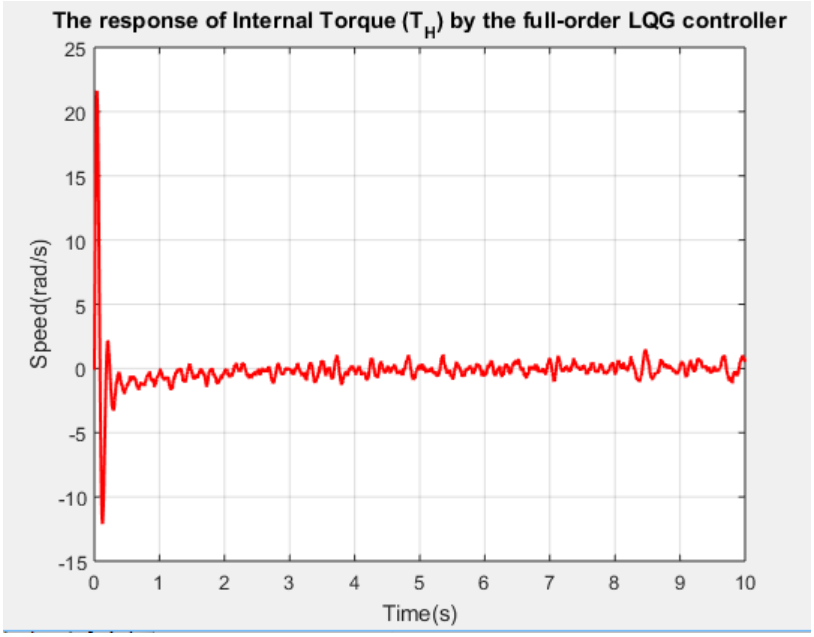

Figure 5.18: Response for (T_H) original system

system for Pitch Angle (β).

Figure 5.26 shows the state estimate for Stator Current (i_d) scaled to proper size for the original system. Figure 5.27 shows the state estimate for Stator Current

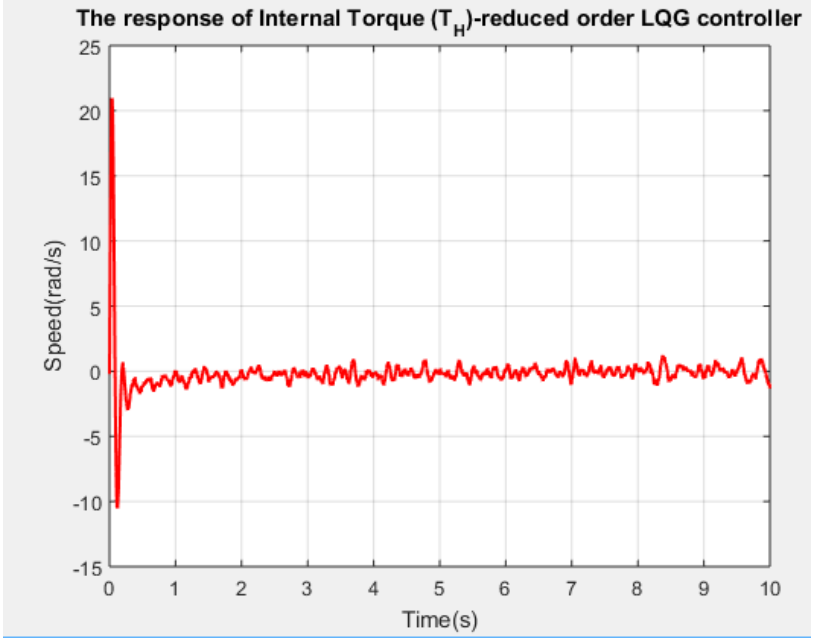

Figure 5.19: Response for (T_H) decomposed system

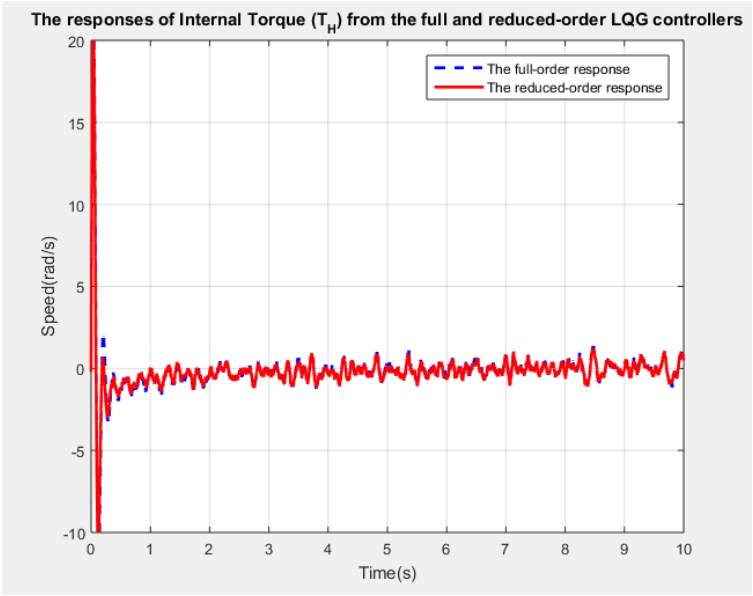

Figure 5.20: Difference between the Responses for (T_H)

(i_d) scaled to proper size for the decomposed system. Figure 5.28 has both of the above graphs for comparison of response for Stator Current (i_d) of original system to that of reduced order system (i.e. Decomposed system). And Figure 5.29 has the

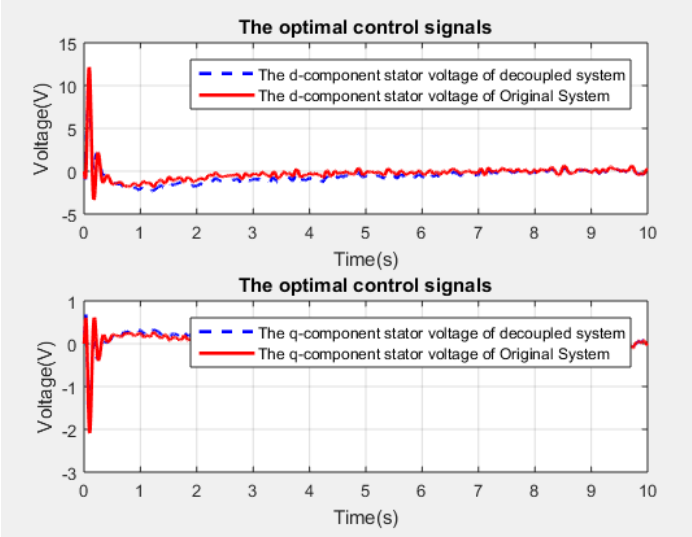

Figure 5.21: Difference between the Control signals for (T_H)

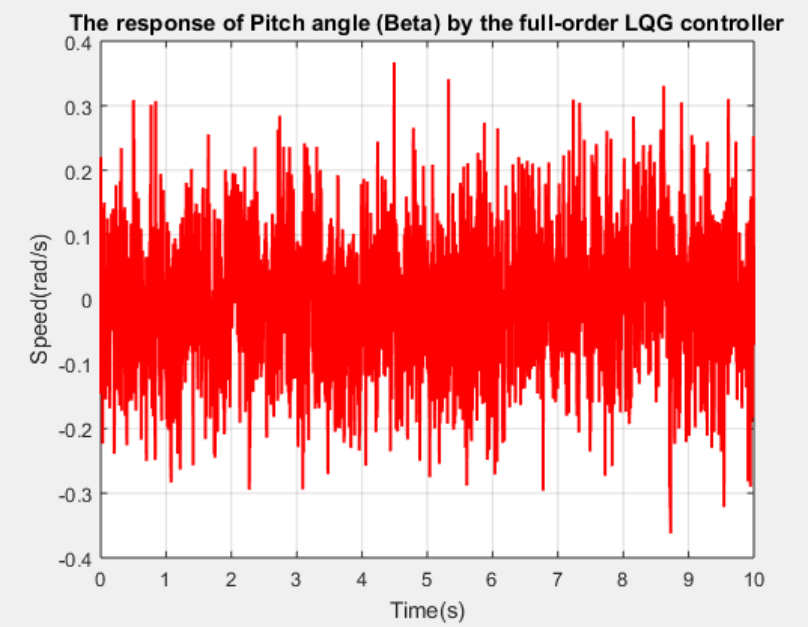

Figure 5.22: Response for (β) original system

difference between control signals generated by LQG control loops of original system and decomposed system for Stator Current (i_d).

Figure 5.30 shows the state estimate for Stator Current (i_q) scaled to proper size for the original system. Figure 5.31 shows the state estimate for Stator Current

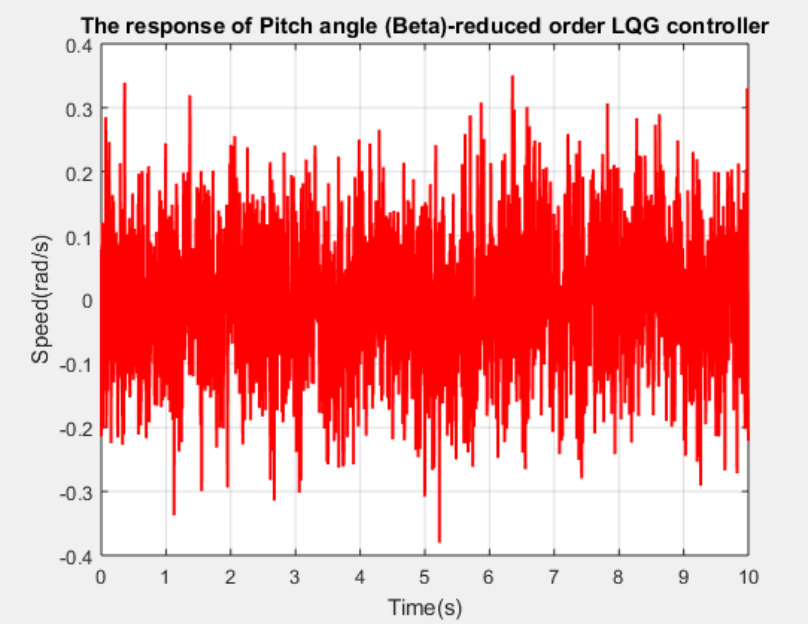

Figure 5.23: Response for (β) decomposed system

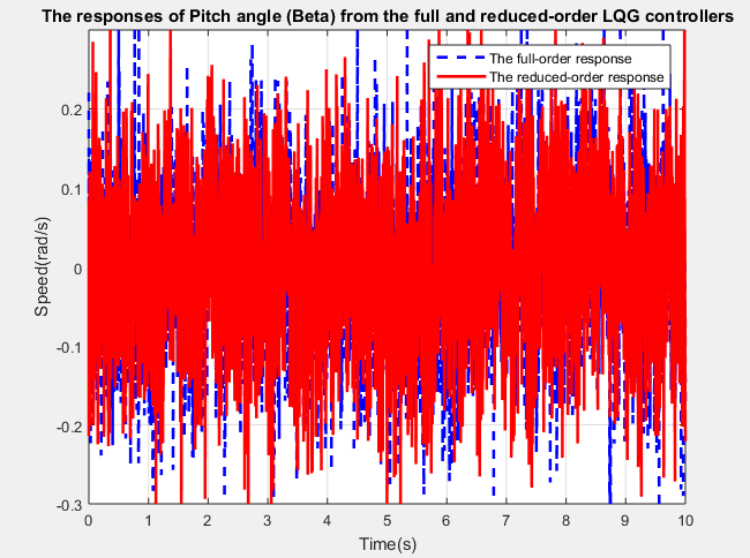

Figure 5.24: Difference between the Responses for (β)

(i_q) scaled to proper size for the decomposed system. Figure 5.32 has both of the above graphs for comparison of response for Stator Current (i_q) of original system to that of reduced order system (i.e. Decomposed system). And Figure 5.33 has the

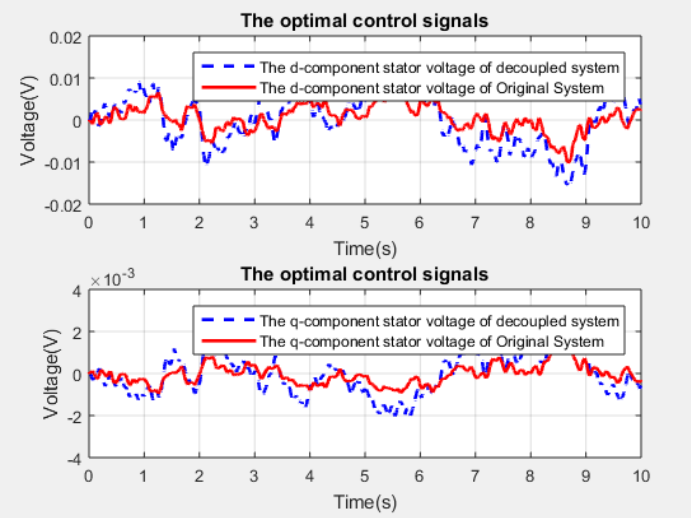

Figure 5.25: Difference between the Control signals for (β)

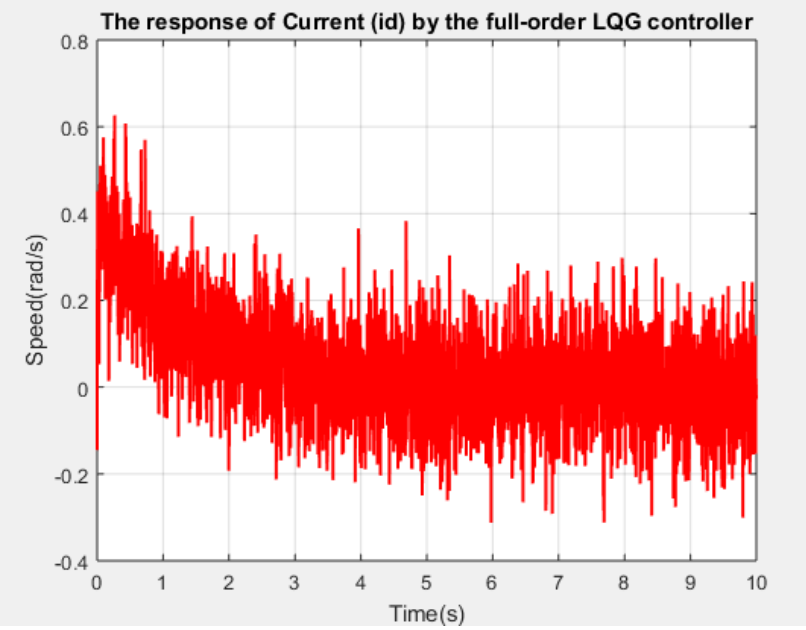

Figure 5.26: Response for (i_d) original system

difference between control signals generated by LQG control loops of original system and decomposed system for Stator Current (i_q).

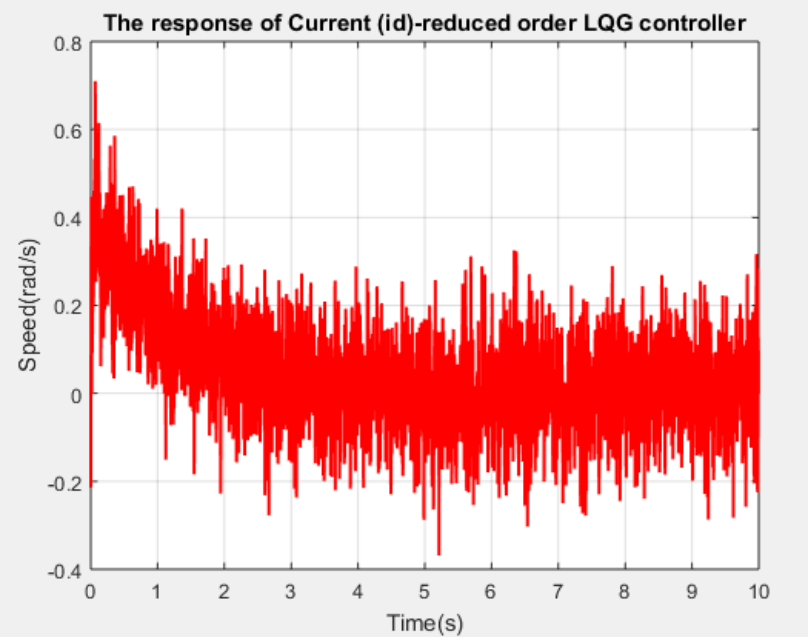

Figure 5.27: Response for (i_d) decomposed system

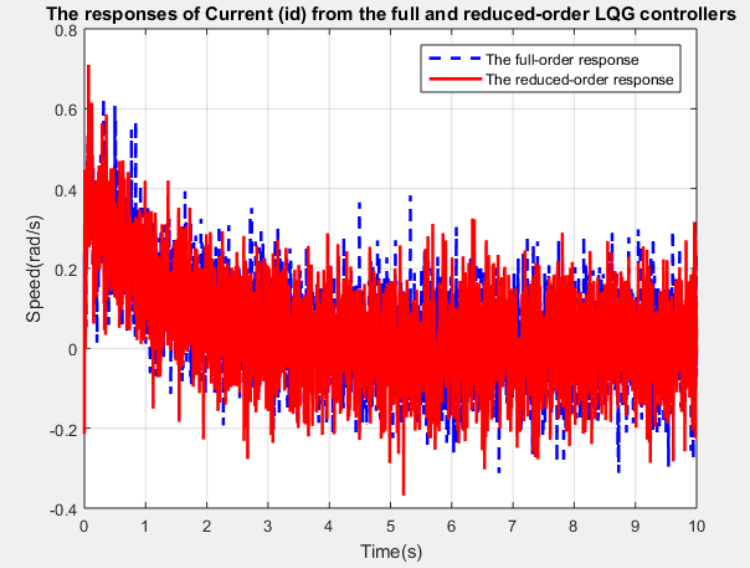

Figure 5.28: Difference between the Responses for (i_d))

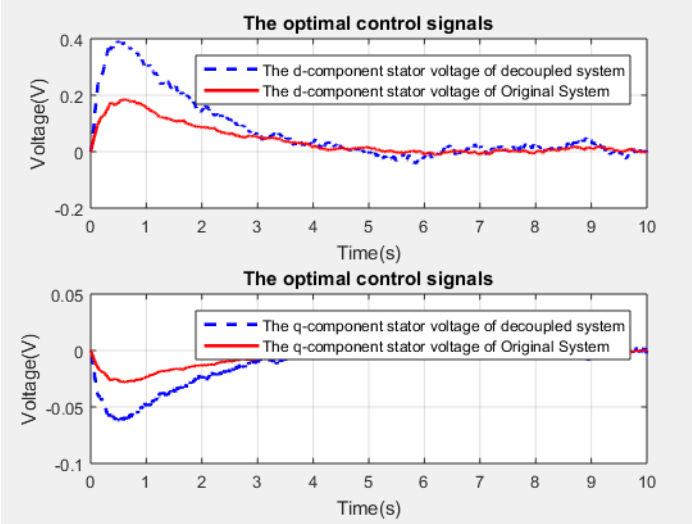

Figure 5.29: Difference between the Control signals for (i_d)

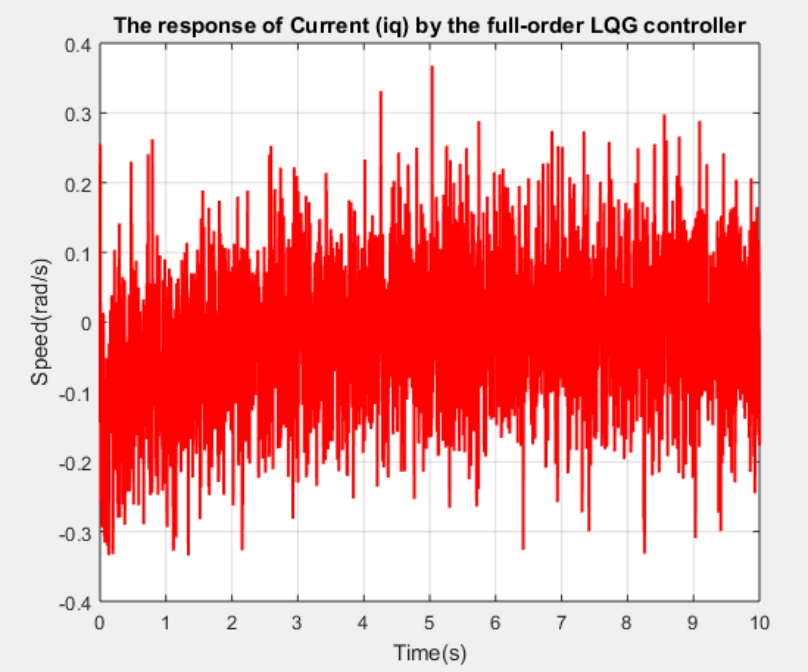

Figure 5.30: Response for (i_q) original system

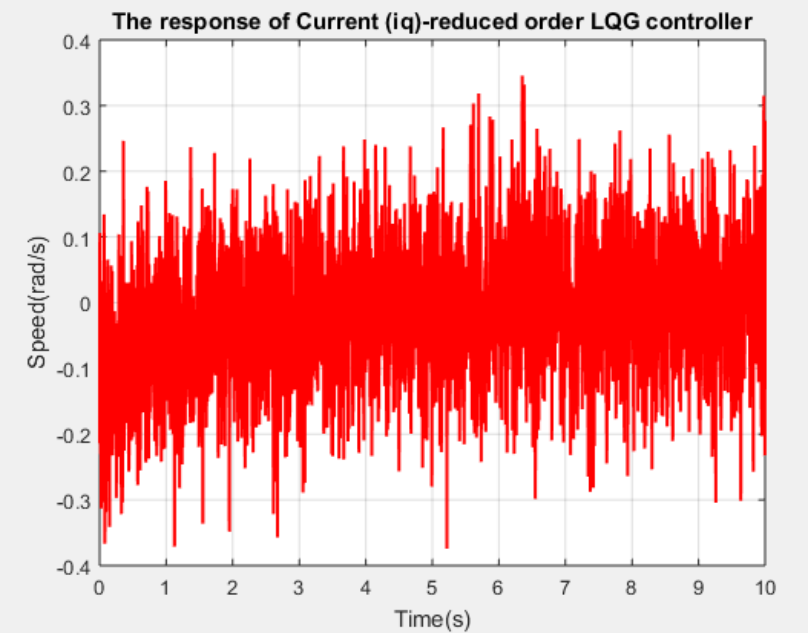

Figure 5.31: Response for (i_q) decomposed system

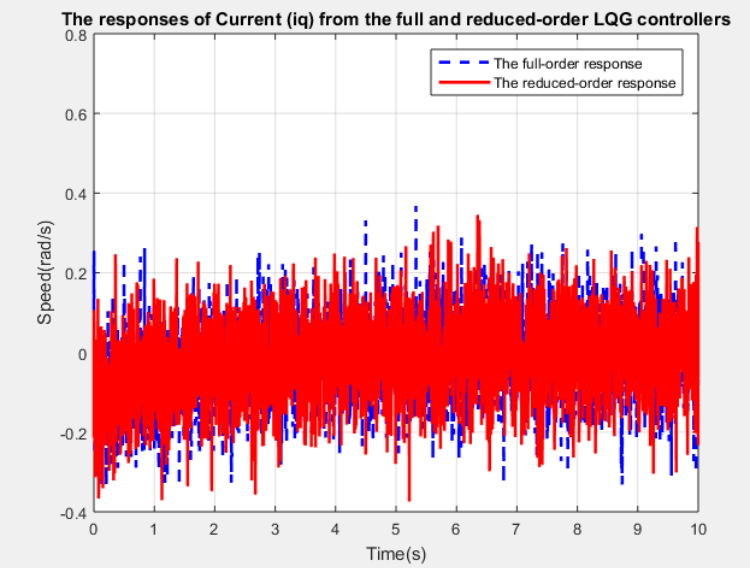

Figure 5.32: Difference between the Responses for (i_q))

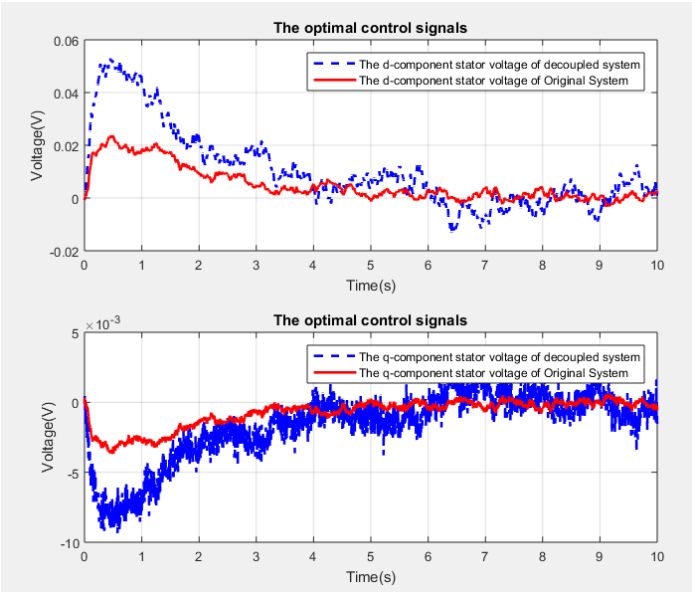

Figure 5.33: Difference between the Control signals for (i_q)

6 Conclusions and Future Works

6.1 Conclusion

Wind energy penetration into the electric grid and electric energy generation is increasing exponentially year after year and control system acts as a brain to WECS dictating it how to behave in different kinds of environment and different weather conditions and also how to change behaviour with the changes in weather conditions, along side of balancing with the noises generated internally and externally and improving the energy conversion efficiency with little to effect to the physical health conditions of the WECS. So, to manage a WECS system to overcome all the above mentioned problems and fulfill the requirements, traditional control techniques are not capable to perform such complex tasks. Therefore, advanced control techniques are needed for fulfilling the needs and managing all the control problems with proper trade-offs that are acceptable, reliable and profitable. In this project optimal control strategies with singular perturbation and time scales methods have been proposed and the conclusions about those techniques and their implementation is summarized below:

1. *Singular Perturbation and Time Scales:* By dividing a single higher order complex system with fast and slow dynamics into two separate subsystems makes the design less complex with lower effort mathematically with flexible inexpensive ways for designing controllers. The results have shown that closeness of results

of subsystem results to that of results of single higher order complex system conclude that the behaviour of the systems does not change in any manner by implementing the time-scales techniques.

2. *LQR optimal control:* Optimal controllers were designed for the Higher-order system and then also for the slow and fast subsystems obtained from the Higher-order system by using singular perturbation and time scales. The performance of the reduced-order slow and fast LQR controllers were compared with original higher-order LQR controller using the simulation results which show that the performance of both are very close to each other.

3. *LQG optimal control:* LQG control technique used in this project is similar to that of LQR control but the systems are assumed to be influenced by the Guassian noises and some system states are unavailable so, Kalman filters are designed to estimate the unavailable states. The designed Kalman filter is separated into slow and fast Kalman filters by using Singular perturbation and time scales technique and combined with slow and fast LQG gains, forming reduced order LQG optimal controllers. And the both the simulation results are compared to verify that the performance of the reduced order LQG filters and higher-order LQG filters are the same. performance.

6.2 Future Works

The responsibility of a control system in WECS has very wide variety of roles as listed out in the problem statement and the area focused in this project is with improvement of conversion efficiency for the VSVP-WECS. The remaining problems have not been addressed in this project so, some of the possible pointers for the future

works related to WECS are as follows:

1. Evolving the modelling of WECS to include other major impacting factors on the performance of WECS.The models derived in this project are much simplified by considering only the fundamental dynamics into account. The other models that could be integrated include much more complex factors like tower bending, phenomenon of wind shear and tower shadowing which induce negative compacts on power output which are not investigated. The next step would be identifying other dynamics that could be integrated into the model to represent the WECS system in more detail mathematically for further studies, using first principle or system identification.

2. Applying of singular perturbation to the non-linear models of WECS. Singular perturbation and time scales have only been implemented on the linear model in this project. The implementation on non-linear systems model would give better results with non-linear dynamics being taken into account.

3. Implementation of advanced control techniques on VSVP-WECS. In this project the implementation of singular perturbation on VSVP-WECS is only done using the optimal control techniques. Other advanced control techniques like adaptive control and other hybrid control techniques could be explored to improve the performance.

References

[1] E. S. Abdin and W. Xu. "Control design and dynamic performance analysis of a wind turbine-induction generator unit". In: *Power System Technology, 1998. Proceedings. POWERCON '98. 1998 International Conference on*. Vol. 2. Aug. 1998, 1198–1202 vol.2. DOI: 10.1109/ICPST.1998.729275 (cit. on p. 32).

[2] S. E. Aimani. "Modeling and control structures for variable speed wind turbine". In: *2011 International Conference on Multimedia Computing and Systems*. Apr. 2011, pp. 1–5. DOI: 10.1109/ICMCS.2011.5945670 (cit. on p. 32).

[3] X. Anjun, X. Hao, H. Shuju, and X. Honghua. "Pitch control of large scale wind turbine based on expert PID control". In: *2011 International Conference on Electronics, Communications and Control (ICECC)*. Sept. 2011, pp. 3836–3839. DOI: 10.1109/ICECC.2011.6068002 (cit. on p. 18).

[4] A. Beainy, C. Maatouk, N. Moubayed, and F. Kaddah. "Comparison of different types of generator for wind energy conversion system topologies". In: *2016 3rd International Conference on Renewable Energies for Developing Countries (REDEC)*. July 2016, pp. 1–6. DOI: 10.1109/REDEC.2016.7577535 (cit. on p. 17).

[5] T. Burton. *Wind Energy Handbook. 2nd Edition*. John Wiley Sons, Ltd., 2011 (cit. on p. 2).

[6] K. W. Chang. "Singular Perturbations of a General Boundary Value Problem". In: *SIAM Journal on Mathematical Analysis* 3.3 (1972), pp. 520–526. DOI: 10.1137/0503050. eprint: https://doi.org/10.1137/0503050. URL: https://doi.org/10.1137/0503050 (cit. on p. 43).

[7] Z. Chen, J. M. Guerrero, and F. Blaabjerg. "A Review of the State of the Art of Power Electronics for Wind Turbines". In: *IEEE Transactions on Power Electronics* 24.8 (Aug. 2009), pp. 1859–1875. ISSN: 0885-8993. DOI: 10.1109/TPEL.2009.2017082 (cit. on p. 17).

[8] G. W. E. Council. "Global Wind Energy Council Report 2016 April". In: (Apr. 2016). URL: http://www.gwec.net/wp-content/uploads/vip/GWEC-Global-Wind-2015-Report_April-2016_22_04.pdf (cit. on pp. 1, 8, 9).

[9] D.S.Naidu. *Optimal Control Systems*. CRC Press, June 2002 (cit. on pp. 19, 59).

[10] ". of Energy Efficiency and R. Energy". "Advantages and Challenges of Wind Energy". In: (). URL: https://energy.gov/eere/wind/advantages-and-challenges-wind-energy (cit. on p. 5).

[11] D. (D. of Energy). "How wind turbine works". In: (Sept. 2011). URL: http://www1.eere.energy.gov/wind/wind_how.html#inside (cit. on pp. 11, 13–15).

[12] G. R. Energy. "Characteristics of Wind-Wind speed pattern". In: (). URL: http://www.greenrhinoenergy.com/renewable/wind/wind_characteristics.php (cit. on p. 2).

[13] M. Ezzat, M. Benbouzid, S. M. Muyeen, and L. Harnefors. "Low-voltage ride-through techniques for DFIG-based wind turbines: state-of-the-art review and

future trends". In: *IECON 2013 - 39th Annual Conference of the IEEE Industrial Electronics Society*. Nov. 2013, pp. 7681–7686. DOI: 10.1109/IECON.2013.6700413 (cit. on p. 17).

[14] H. a. FernandoD.Bianchi. *Wind Turbine Control Systems. Principles, Modelling and Gain scheduling design, 1st edition*. Springer-Verlag, 2007 (cit. on pp. 4, 37).

[15] M. Fliess and C. Join. "Intelligent PID controllers". In: *2008 16th Mediterranean Conference on Control and Automation*. June 2008, pp. 326–331. DOI: 10.1109/MED.2008.4601995 (cit. on pp. 18, 19).

[16] Z. Gajic and M. Lim. *Optimal control of singularly perturbed linear systems and applications*. Marcel Dekker, Inc., 2001 (cit. on pp. 48, 65, 70).

[17] H. Geng and G. Yang. "Robust pitch controller for output power levelling of variable-speed variable-pitch wind turbine generator systems". In: *IET Renewable Power Generation* 3.2 (June 2009), pp. 168–179. ISSN: 1752-1416. DOI: 10.1049/iet-rpg:20070043 (cit. on pp. 21, 22).

[18] T. Grodt and Z. Gajic. "The recursive reduced-order numerical solution of the singularly perturbed matrix differential Riccati equation". In: *IEEE Transactions on Automatic Control* 33.8 (Aug. 1988), pp. 751–754. ISSN: 0018-9286. DOI: 10.1109/9.1291 (cit. on p. 48).

[19] M. P. S. Gryning, Q. Wu, M. Blanke, H. H. Niemann, and K. P. H. Andersen. "Wind Turbine Inverter Robust Loop-Shaping Control Subject to Grid Interaction Effects". In: *IEEE Transactions on Sustainable Energy* 7.1 (Jan. 2016), pp. 41–50. ISSN: 1949-3029. DOI: 10.1109/TSTE.2015.2472285 (cit. on pp. 21, 22).

[20] X. f. Huang, D. Luo, G. q. Wang, N. Ding, J. r. Xu, Y. Liu, and H. Fan. "State of the Art in Condition Monitoring in Wind Turbines Based on Embedded FBG Sensors". In: *2010 Asia-Pacific Power and Energy Engineering Conference*. Mar. 2010, pp. 1–4. DOI: 10.1109/APPEEC.2010.5448939 (cit. on p. 17).

[21] J. Hussain and M. K. Mishra. "Adaptive Maximum Power Point Tracking Control Algorithm for Wind Energy Conversion Systems". In: *IEEE Transactions on Energy Conversion* 31.2 (June 2016), pp. 697–705. ISSN: 0885-8969. DOI: 10.1109/TEC.2016.2520460 (cit. on p. 23).

[22] E. C. Iulian Munteanu Antoneta Iuliana Bratcu Nicolaos-Antonio Cutululis. "Design Methods for WECS Optimal Control with Energy Efficiency Criterion". In: *Optimal Control of Wind Energy Systems*. Ed. by P. o. I. S. Professor Michael J. Grimble, P. (o. C. S. Director Professor Michael A. Johnson, and D. Director. Salmon Tower Building, New York City, USA: Springer-Verlag London Limited, 2008. Chap. 5, pp. 109–166. ISBN: 978-1-84800-079-7. DOI: 10.1007/978-1-84800-080-3 (cit. on p. 19).

[23] E. C. Iulian Munteanu Antoneta Iuliana Bratcu Nicolaos-Antonio Cutululis. *Optimal Control of Wind Energy Systems. Towards a Global Approach*. Springer-Verlag, 2006. ISBN: 978-1-84800-079-7 (cit. on p. 42).

[24] E. Iyasere, D. M. Dawson, J. R. Wagner, M. Salah, and E. Tatlicioglu. "Nonlinear robust control to maximize energy capture in a variable speed wind turbine using an induction generator". In: *2009 IEEE International Conference on Systems, Man and Cybernetics*. Oct. 2009, pp. 4071–4076. DOI: 10.1109/ICSMC.2009.5346675 (cit. on p. 22).

[25] H. Jafarnejadsani, J. Pieper, and J. Ehlers. "Adaptive Control of a Variable-Speed Variable-Pitch Wind Turbine Using Radial-Basis Function Neural Network". In: *IEEE Transactions on Control Systems Technology* 21.6 (Nov. 2013), pp. 2264–2272. ISSN: 1063-6536. DOI: 10.1109/TCST.2012.2237518 (cit. on p. 23).

[26] P. Kokotovic. "A Riccati equation for block-diagonalization of ill-conditioned systems". In: *IEEE Transactions on Automatic Control* 20.6 (Dec. 1975), pp. 812–814. ISSN: 0018-9286. DOI: 10.1109/TAC.1975.1101089 (cit. on p. 48).

[27] M. Koumir, A. E. Bakri, and I. Boumhidi. "Optimal control for a variable speed wind turbine based on extreme learning machine and adaptive Particle Swarm Optimization". In: *2016 5th International Conference on Systems and Control (ICSC)*. May 2016, pp. 151–156. DOI: 10.1109/ICoSC.2016.7507047 (cit. on p. 20).

[28] S. Li, H. Wang, Y. Tian, and A. Aitouche. "A sliding model control based on intelligent PID control for wind turbine system". In: *2015 4th International Conference on Systems and Control (ICSC)*. Apr. 2015, pp. 255–260. DOI: 10.1109/ICoSC.2015.7152776 (cit. on p. 18).

[29] Y. Li, Z. Xu, and K. Meng. "Optimal Power Sharing Control of Wind Turbines". In: *IEEE Transactions on Power Systems* 32.1 (Jan. 2017), pp. 824–825. ISSN: 0885-8950. DOI: 10.1109/TPWRS.2016.2549741 (cit. on pp. 20, 21).

[30] A. McIver, D. G. Holmes, and P. Freere. "Optimal control of a variable speed wind turbine under dynamic wind conditions". In: *Industry Applications Conference, 1996. Thirty-First IAS Annual Meeting, IAS '96., Conference Record of the 1996 IEEE*. Vol. 3. Oct. 1996, 1692–1698 vol.3. DOI: 10.1109/IAS.1996.559297 (cit. on p. 19).

[31] E. B. Muhando, T. Senjyu, E. Omine, and T. Funabashi. "Full state feedback digital control of WECS with state estimation by stochastic modeling design". In: *2008 IEEE Power and Energy Society General Meeting - Conversion and Delivery of Electrical Energy in the 21st Century*. July 2008, pp. 1–8. DOI: 10.1109/PES.2008.4596132 (cit. on p. 32).

[32] E. B. Muhando, T. Senjyu, E. Omine, T. Funabashi, and C.-H. Kim. "Functional modeling for intelligent controller design for MW-class variable speed wecs with independent blade pitch regulation". In: *2008 IEEE 2nd International Power and Energy Conference*. Dec. 2008, pp. 413–418. DOI: 10.1109/PECON.2008.4762508 (cit. on p. 32).

[33] A. Murdoch, J. R. Winkelman, S. H. Javid, and R. S. Barton. "Control Design and Performance Analysis of a 6 MW Wind Turbine-Generator". In: *IEEE Power Engineering Review* PER-3.5 (May 1983), pp. 49–49. ISSN: 0272-1724. DOI: 10.1109/MPER.1983.5519172 (cit. on p. 32).

[34] D. S. Naidu. "Singular perturbations and Time Scales in Control Theory and Applications: An Overview". In: *Dynamics of Continuous, Discrete and Impulsive Systems Series B: Applications Algorithms* 9, Number 2 (2002), pp. 233–278 (cit. on pp. 43, 59).

[35] D. S. Naidu. *Singular Perturbation Methodology in Control Systems. 1st Edition*. Peter Peregrinus Ltd., 1998 (cit. on pp. 43, 48, 59).

[36] H. M. Nguyen and D. S. Naidu. "Advanced control strategies for wind energy systems: An overview". In: *2011 IEEE/PES Power Systems Conference and Exposition*. Mar. 2011, pp. 1–8. DOI: 10.1109/PSCE.2011.5772514 (cit. on p. 17).

[37] H. M. Nguyen and D. S. Naidu. "Time scale analysis and control of Wind Energy Conversion Systems". In: *2012 5th International Symposium on Resilient Control Systems*. Aug. 2012, pp. 149–154. DOI: 10.1109/ISRCS.2012.6309309 (cit. on pp. 43, 59).

[38] H. Nguyen and D. S. Naidu. "Evolution of Wind Turbine Control Systems". In: *Encyclopedia of Life Support Systems*. Oxford ,UK: UNESCO, EOLSS, 2013 (cit. on p. 29).

[39] N. P. Prabhu, P. Yadav, B. Prasad, and S. K. Panda. "Optimal placement of offshore wind turbines and subsequent micro-siting using Intelligently Tuned Harmony Search algorithm". In: *2013 IEEE Power Energy Society General Meeting*. July 2013, pp. 1–7. DOI: 10.1109/PESMG.2013.6673059 (cit. on p. 17).

[40] L. Saihi and A. Boutera. "Robust control of a variable-speed wind turbine with fixed pitch angle and strategy MPPT control associated on a PMSG". In: *2016 8th International Conference on Modelling, Identification and Control (ICMIC)*. Nov. 2016, pp. 326–331. DOI: 10.1109/ICMIC.2016.7804131 (cit. on pp. 21, 22).

[41] A. P. Schaffarczyk. *Introduction to Wind Turbine Aerodynamics*. Springer Verlag, 2014. Chap. Types of Wind Turbines. ISBN: 978-3-642-36408-2. URL: http://www.springer.com/us/book/9783642364082 (cit. on p. 13).

[42] M. Soliman, O. P. Malik, and D. T. Westwick. "Multiple model multiple-input multiple-output predictive control for variable speed variable pitch wind energy conversion systems". In: *IET Renewable Power Generation* 5.2 (Mar. 2011), pp. 124–136. ISSN: 1752-1416. DOI: 10.1049/iet-rpg.2009.0137 (cit. on p. 37).

[43] S. Toledo, M. Rivera, and J. L. Elizondo. "Overview of wind energy conversion systems development, technologies and power electronics research trends". In: *2016 IEEE International Conference on Automatica (ICA-ACCA)*. Oct. 2016, pp. 1–6. DOI: 10.1109/ICA-ACCA.2016.7778454 (cit. on p. 17).

[44] N. Ullah, M. A. Ali, A. Ibeas, and J. Herrera. "Adaptive Fractional Order Terminal Sliding Mode Control of a Doubly Fed Induction Generator-Based Wind Energy System". In: *IEEE Access* 5 (2017), pp. 21368–21381. DOI: 10.1109/ACCESS.2017.2759579 (cit. on p. 23).

[45] M. Vali, J. W. van Wingerden, and M. Khn. "Optimal multivariable individual pitch control for load reduction of large wind turbines". In: *2016 American Control Conference (ACC)*. July 2016, pp. 3163–3169. DOI: 10.1109/ACC.2016.7525404 (cit. on p. 20).

[46] W. Wang, D. Wu, Y. Wang, and Z. Ji. "H$gainschedulingcontrolofPMSG-basedwindpowerconversionsystem$". In: *2010 5th IEEE Conference on Industrial Electronics and Applications*. June 2010, pp. 712–717. DOI: 10.1109/ICIEA.2010.5516964 (cit. on p. 22).

[47] N. W. Watch. *Physical Size and Area Needed for a typical WECS*. Wind watch Inc. URL: https://www.wind-watch.org/faq-size.php (cit. on p. 10).

[48] R. Wiser. "Low Wind Energy Price and Growing Wind Energy in US". In: (). URL: http://www.renewableenergyworld.com/articles/2015/08/us-wind-energy-selling-at-record-low-price-of-2-5-cents-per-kwh.html (cit. on p. 5).

[49] V. Yaramasu, B. Wu, M. Rivera, and J. Rodriguez. "A New Power Conversion System for Megawatt PMSG Wind Turbines Using Four-Level Converters and a Simple Control Scheme Based on Two-Step Model Predictive Strategy; Part I:

Modeling and Theoretical Analysis". In: *IEEE Journal of Emerging and Selected Topics in Power Electronics* 2.1 (Mar. 2014), pp. 3–13. ISSN: 2168-6777. DOI: 10.1109/JESTPE.2013.2294920 (cit. on p. 24).

[50] D. Yu, M. S. Li, T. Y. Ji, and Q. H. Wu. "Optimal voltage control of power systems with uncertain wind power using FACTS devices". In: *2016 IEEE Innovative Smart Grid Technologies - Asia (ISGT-Asia)*. Nov. 2016, pp. 937–941. DOI: 10.1109/ISGT-Asia.2016.7796511 (cit. on p. 17).

[51] Y. Zhang, D. S. Naidu, H. M. Nguyen, C. Cai, and Y. Zou. "Time scale analysis and synthesis for Model Predictive Control under stochastic environments". In: *2014 7th International Symposium on Resilient Control Systems (ISRCS)*. Aug. 2014, pp. 1–6. DOI: 10.1109/ISRCS.2014.6900085 (cit. on p. 43).

[52] H. Zhao, Q. Wu, Q. Guo, H. Sun, and Y. Xue. "Distributed Model Predictive Control of a Wind Farm for Optimal Active Power ControlPart I: Clustering-Based Wind Turbine Model Linearization". In: *IEEE Transactions on Sustainable Energy* 6.3 (July 2015), pp. 831–839. ISSN: 1949-3029. DOI: 10.1109/TSTE.2015.2418282 (cit. on p. 24).